Åbo Akademi University

Hossein Vakili

Application of Analytical Techniques in Quality Control of Printed Pharmaceutical Dosage Forms

A Study in Pharmaceutical Sciences

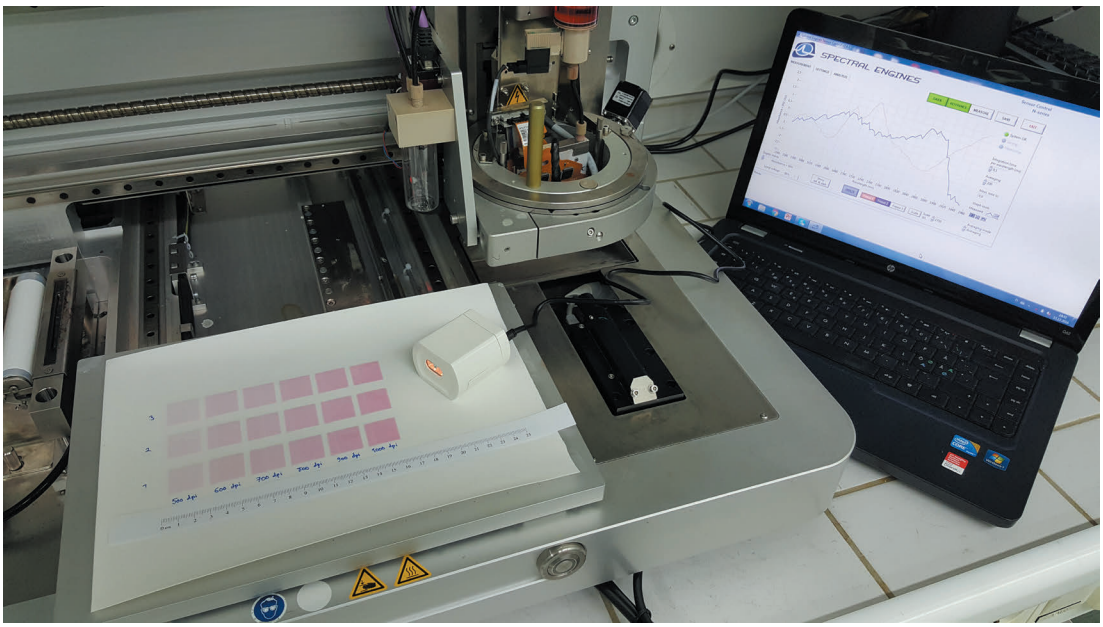

A tailor-made dose suits you best.

Hossein Vakili

Born 1984 in Tehran, Iran

B.Sc. Petroleum Engineering - Production
at Petroleum University of Technology (Iran) in 2007

M.Sc. Chemical Engineering - Analytical Chemistry
at Åbo Akademi University in 2012

Cover image: A series of printed dosage forms manufactured by a PixDro LP50 piezoelectric inkjet printer and a compact near infra-red spectrometer connected to a personal computer for quality control of the final medicinal products.

Application of analytical techniques in quality control of printed pharmaceutical dosage forms

A study in Pharmaceutical Sciences

Hossein Vakili

Pharmaceutical Sciences Laboratory
Faculty of Science and Engineering
Åbo Akademi University
Åbo, Finland, 2018

Supervisors

Professor Niklas Sandler, PhD
Pharmaceutical Sciences Laboratory
Åbo Akademi University
Finland

Professor Johan Bobacka, PhD
Laboratory of Analytical Chemistry
Åbo Akademi University
Finland

Assistant Professor Natalja Genina, PhD
Pharmaceutical Technology and Engineering
University of Copenhagen
Denmark

Reviewers

Professor Clare Strachan, PhD
Faculty of Pharmacy
University of Helsinki
Finland

Professor Maike Windbergs, PhD
Buchmann Institute for Molecular Life Sciences
Goethe University Frankfurt
Germany

Opponent

Professor Clare Strachan, PhD
Faculty of Pharmacy
University of Helsinki
Finland

ISBN 978-952-12-3658-7 (PRINT)
ISBN 978-952-12-3659-4 (PDF)
Painosalama Oy, Turku, Finland 2018

Table of contents

Abstract

There is a need for development and production of pharmaceutical dosage forms with flexible dosing in order to achieve the essential requirements of precision medicine for patient-specific therapy. Precision medicine implicates a paradigm shift towards a new perspective both in clinical practice to include patients' individual characteristics in a more personalized diagnosis of the disease and subsequently in formulation design and manufacturing of the tailored dosage forms for an optimal and well-tolerated therapeutic treatment.

From the drug delivery perspective, adoption of new technologies that provide dose flexibility in small batch productions has been regarded as key for on-demand production of tailored medicines for late-stage delivery at envisaged point-of-care such as in hospitals or pharmacy settings. In this regard, inkjet printing technology has been proposed in the past decade as the method that is capable of depositing extremely accurate, low and uniform amounts of drugs on various edible polymeric films which is currently being further investigated by researchers. Today, the state of the art inkjet printers with compact design, open architecture and advanced integrated visualization systems provide thorough control over the shape, size, alignment and spatial deposition of thousands of single drops in picoliter range in pixel-wise accuracy onto the printing substrates. Printed pharmaceuticals are often in the form of orodispersible formulations that rapidly dissolve in the mouth resulting in ease of administration and higher patient compliance especially for pediatrics and those with swallowing inabilities and disorder. In this way, when the drug is properly absorbed through the oral mucosa, it avoids first-pass metabolism in the liver and directly enters the systemic circulation and starts a fast onset of actions.

One of the main problems in the way of inkjet printing technology becoming a genuine, viable and commonly accepted method by regulatory agencies for continuous manufacturing of solid dosage forms is the lack of rapid, robust, reliable and most importantly non-invasive analytical techniques for real-time quality control of the printed formulations. This thesis was mainly focused on exploring a variety of analytical techniques and small-size instrumentations for the study of drug content, uniformity of drug distribution and drug release profile from the printed units.

Ion-selective electrodes were designed for continuous monitoring of the drug release from porous cellulose substrates and thin films as an attempt to propose a cost-effective and efficient alternative to conventional time and labor-intensive methods. Flexographic printing technique was used for applying several layers of highly viscous and insoluble polymeric coating on already inkjet printed formulations to achieve formulations with modified release profiles. Near-infrared

(NIR) hyperspectral imaging was applied to predict the drug amount and to create concentration distribution maps that offer both statistical and visual assessments of the printed formulations. The feasibility of a compact colorimetric device was investigated in CIELAB color space for indirect estimation of the drug content in pediatric orodispersible formulations. Finally, a handheld NIR spectrometer was used together with advanced chemometrics to build predictive models for drug content analysis and classification of the dosage forms containing two poorly water soluble drugs. In addition, the application of multivariate data analysis techniques for processing and modeling of the spectroscopic data were discussed in detail. Several other analytical techniques were also applied to study the surface morphology, surface roughness, texture, mechanical properties and disintegration behavior of the raw and printed substrates together with solid-state characteristics and the stability of the inks and the drugs in formulations. The advantages and shortcomings of each formulation design and applied analytical method were highlighted and a general approach for future complimentary studies was proposed.

This research provides a deeper insight into the inkjet printing process of drug formulations and subsequently inspects the feasibility of the proposed analytical probes as fast, reliable and non-invasive quality control tools at the production line in search for bringing the concept of personalized medicine closer to reality.

List of original publications

This thesis is based on the following publications which are referred to in the text by their corresponding Roman numbers (I-V).

I. **Vakili, H.**, Genina, N., Ehlers, H., Bobacka, J., Sandler, N. (2012). Using ion-selective electrodes to study the drug release from porous cellulose matrices. *Pharmaceutics*, 4 (3), 366–376.

II. Genina, N., Fors, D., **Vakili, H.**, Ihalainen, P., Pohjala, L., Ehlers, H., Kassamakov, I., Haeggstrom, E., Vuorela, P., Peltonen, J., Sandler, N. (2012). Tailoring controlled-release oral dosage forms by combining inkjet and flexographic printing techniques. *European Journal of Pharmaceutical Sciences*, 47 (3), 615–623.

III. **Vakili, H.**, Kolakovic, R., Genina, N., Marmion, M., Salo, H., Ihalainen, P., Peltonen, J., Sandler, N. (2015). Hyperspectral imaging in quality control of inkjet printed personalised dosage forms. *International Journal of Pharmaceutics*, 483 (1-2), 244–249.

IV. **Vakili, H.**, Nyman, J.O., Genina, N., Preis, M., Sandler, N., (2016). Application of a colorimetric technique in quality control for printed pediatric orodispersible drug delivery systems containing propranolol hydrochloride. *International Journal of Pharmaceutics*, 511 (1), 606–618.

V. **Vakili, H.**, Wickström, H., Desai, D., Preis, M., Sandler, N. (2017). Application of a handheld NIR spectrometer in prediction of drug content in inkjet printed orodispersible formulations containing prednisolone and levothyroxine. *International Journal of Pharmaceutics*, 524 (1-2), 414–423.

Contribution of **Hossein Vakili** to the original publications:

I. Participation in the study design; performing the experiments and data analysis; writing the paper.

II. Participation in the study design; performing a part of experiments; reviewing the manuscript.

III. Participation in the study design; performing part of the experiments and all of data analysis; writing the paper.

IV. Participation in the study design; performing the experiments and data analysis; writing the paper.

V. Participation in the study design; performing most of the experiments and all of data analysis; writing the paper.

Abbreviations

2D	Two-dimensional
3D	Three-dimensional
API	Active pharmaceutical ingredient
ATR-IR	Attenuated total reflectance infrared spectroscopy
BCS	Biopharmaceutics Classification System
CERP	Coated edible rice paper
CIE	Commission International d'Eclairage
CSDD	Center for the study of drug development
d_v90	Volume distribution value
DAMPP	Dropwise additive manufacturing of pharmaceutical products
DoE	Design of experiment
DSC	Differential scanning calorimetry
EC	Ethyl cellulose
EDX	Energy-dispersive X-ray analysis
EIS	Edible icing sheet
EMA	European medicine agency
EMF	Electromotive force
ERP	Edible rice paper
FDA	United States Food and Drug Administration
GIT	Gastrointestinal tract
GMP	Good Manufacturing Practice
HGP	Human Genome Project
HPC	Hydroxypropyl cellulose
HPLC	High performance liquid chromatography
HPMC	Hydroxypropyl methyl cellulose
ISEs	Ion-Selective Electrodes
IUPAC	International Union of Pure and Applied Chemistry
KTFPB	Potassium tetrakis[3,5-bis(trifluoromethyl)phenyl]borate
KTpClPB	Potassium tetrakis(4-chlorophenyl) borate
MEC	Minimum effective concentration
mid-IR	Middle-infrared
MSC	Multiplicative scatter correction
MTC	Minimum toxic concentration
NIR	Near-infrared
NME	New molecular entities
NPOE	2-nitrophenyl octyl ether
NRC	National Research Council

NTI	Narrow therapeutic index
ODF	Orodispersible film
OPLS	Orthogonal projections to latent structures
OTC	Over-the-counter
PAT	Process Analytical Technology
PC	Principal component
PCA	Principal component analysis
PEG	Polyethylene glycol
PET	Polyethylene terephthalate
Ph. Eur.	European Pharmacopoeia
PG	Propylene glycol
PLS	Partial least squares
PMI	Precision Medicine Initiative
PVC	Polyvinyl chloride
Q^2	The goodness of prediction
QbD	Quality by Design
R^2	Correlation coefficient
RH	Relative humidity
RMSE*cv*	Root mean square error of cross–validation
RMSEE	Root mean square error of estimation
RSP	Riboflavin sodium phosphate
SD	Standard deviation
SDFs	Solid dosage forms
SEM	Scanning electron microscopy
SG	Savitzky–Golay
SNV	standard normal variate
SWLI	Scanning white light interferometry
THF	Tetrahydrofuran
UV	Ultraviolet
UV-Vis	Ultraviolet-visible

1. Introduction

'Drug delivery' refers to approaches and tactics to encapsulate an active pharmaceutical ingredient (API), which is the drug compound, into a 'dosage form' which is the final pharmaceutical product that is administrated to a human or animal body through various routes. Many considerations are made in order to achieve a desired therapeutic effect in a balance with minimized side effects of drug consumption.

The route of administration and the nature of the delivery system dictate the patient compliance and adherence to the medical treatment. Oral route is the most common and convenient route for drug delivery. However, a great number of patients have experienced difficulties regarding swallowing large solid dosage forms (SDFs) such as tablets and capsules. Such conventional dosage forms are produced in large batch productions during many tedious steps and finally come only in a few fixed doses to the market. In order to reach the desired flexible dose, a tablet needs to be divided into pieces, which in turn is prone to more dose variations and damage to the integrity of the dosage form which was carefully formulated for a specific delivery purpose. In addition, many drugs when taken orally are metabolized extensively when exposed to the gastrointestinal tract (GIT) and mostly in the liver so that usually a greater dose than needed should be administered which can be harmful.

On the other hand, about 40% of current market approved drugs and nearly 90% of all new molecular entities (NME) are reported to be poorly water soluble. Such drugs have an aqueous solubility of less than 100 μg/ml and depending on their lipid permeability or lipophilic characterization, they belong to the class II or class IV of the Biopharmaceutics Classification System (BCS). From the drug delivery standpoint, the main challenge of modern pharmaceutical industry is to formulate such drugs into various dosage forms through different strategies in order to enhance the water solubility, the dissolution rate and subsequently bioavailability of the formulations. Moreover, there are many highly potent drugs with narrow therapeutic index (NTI) that require careful dose adjustment to avoid severe adverse effects of possible over dosing and the lack of therapeutic effects in case of under dosing. In addition, the required dose for specific patient populations such as pediatrics depends on patient's weight which is subjected to variation. The delivery challenges become even greater when not only very low and uniform doses of such drugs need to be present in the formulations, but also the allowance for dose flexibility needs to be considered as well.

Considering all the factors above, the application of inkjet printing technology has been studied as an innovative approach for design and delivery of new formulations with precise dosing flexibility of many poorly water soluble and narrow therapeutic index drugs in small and cost-effective batch productions. The printed formulations are typically easier to manufacture since there are many fewer steps in the production line. Such dosage forms optimally offer higher compliance when taken orally with discreet administration, fast disintegration in the mouth without the need to drink water and the opportunity to introduce the drug directly to the systemic circulation.

Due to the novelty of inkjet printing technique in the pharmaceutical field and restrictive regulatory conditions, no definitive approaches have been established and implemented to date for inkjet printing in the guidelines to define Good Manufacturing Practice (GMP) requirements or outline Process Analytical Technology (PAT) tools to ensure Quality by Design (QbD) principle for printing delivery systems. Similarly, the application of proper analytical techniques for quality control of such newly designed products needs to be recognized and regulated as well. Current established analytical methods such as ultraviolet-visible (UV-Vis) spectroscopy, High performance liquid chromatography (HPLC) and mass spectroscopy apart from their bulky, complicated and expensive machinery that require intensive labor and maintenance face other restrictions especially in case of a fast work flow and costly samples which need to be pretreated and destroyed when analyzed during a lengthy procedure.

For clear reasons, it was envisioned that application of reliable, small-scale and non-intrusive analytical tools for automated on-, at and in-line monitoring and quality assessment of the final printed products would be a timely approach for the missing puzzle in promotion of inkjet printing technology as a continuous method for official adoption and authorization in pharmaceutical industries and pharmaceutical manufacturing in general. Therefore, efforts have been made in this thesis to explore the applicability of a number of analytical tools to gain a deeper understanding about their advantages and limitations for quality control of printed formulations to pave the way for inkjet printing to become authorized as the forefront of manufacturing and delivery of new medicines for ultimate goal of individualized therapy.

2. Literature overview

2.1. Personalized/precision medicine

Clinicians have been observing since ancient times that patients with similar symptoms may suffer from different illnesses initiated by different causes. Today, the medical care and treatment approaches towards such apparently similar symptoms should be tailored to take into account the individual characteristics of the patients that may have caused the disease. In this way, the therapeutic outcome would be more efficient and beneficial for all the patients' populations regardless of their vast differences in physiological conditions.

The general approach of 'one-size-fits-all' as the 'standard of care' based on the common clinical indications has been practiced commonly in the manufacturing of pharmaceutical products for the treatment of the 'average patient'. The therapeutic approach of 'personalized medicine' or 'precision medicine' has been developed to address the shortcomings of the traditional model and to transform the paradigm of medicinal practice by allowing a patient's individual information to play its crucial role in the search for optimal course of medical treatment. For this to become reality, the pharmaceutical industry should adapt accordingly in order to find practical solutions for design and development of patient-specific formulations in small-scale production settings.

The term personalized medicine was first published by Langreth and Waldholz (1999) in *The Wall Street Journal* even though some of the underlying concepts could be traced back to the early 1960s (Jain, 2002). In the new millennium, the worldwide research interest on the topic has been increasing considerably which is reflected in the number of articles published related to the terms 'personalized medicine' and 'precision medicine' in PubMed library of medicine **(Figure 1)**.

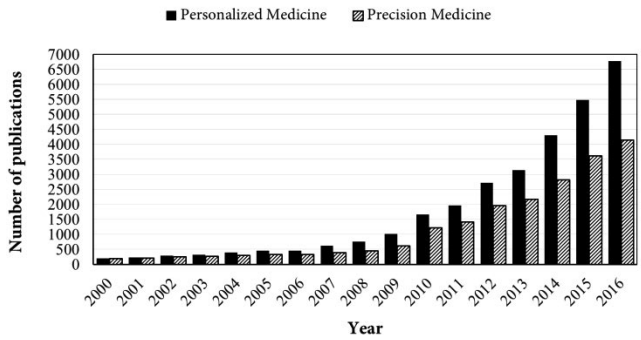

Figure 1. *The number of publications per year in the new millennium related to the terms "personalized medicine" and 'Precision Medicine'. Data were obtained on a PubMed search in March 2017.*

It is necessary to understand that 'personalized medicine' does not refer to unique treatments for each individual as the term might suggest, but rather optimization of pharmaceutical treatment and future illness preventions based on patient characteristics such as genetic and genomic differences, age, gender, race, metabolic capacity, anatomical and physiological features, history of prior treatments, environmental factors, lifestyles, etc. In the European Union, personalized medicine is described as 'providing the right treatment to the right patient, at the right dose at the right time'. The National Research Council (NRC) favors the term 'precision medicine' over 'personalized medicine'; however, both terms are used interchangeably today.

The Human Genome Project (HGP) was reported to have successfully completed the mapping of the human genome in 2003 discovering that the great variation in the human species when exposed to a disease was related to only 0.9% inter-individual genetic differences while 99.1% of the genetic make-up of humans was identical (Novelli, 2010). Genetic and genomic differences could affect the individual responses to specific drug therapies and regulate the minimum effective concentration (MEC) and minimum toxic concentration (MTC) of a drug; therefore, playing an important role in the rate of drug absorption, distribution and elimination in the body (Mallal et al., 2002; Wesołowska-Andersen).

However, this thesis is not focused on pharmacogenomics and genetic variations in metabolic pathways of patients, but it is rather dedicated to exploring *flexible dosing* opportunities in enhanced delivery systems given the needs of precision medicine for different patient populations, e.g. infants, children, adolescents, the elderly. The importance and necessity of personalized medicine for successful age–appropriate therapy has been discussed extensively in the literature (Breitkreutz and Boos, 2007; Visser et al., 2017). The therapeutic dose for pediatric patients is usually calculated based on the weight or body volume of the child which is subjected to variation; therefore, a wider selection of dose strengths should be available for successful therapeutic outcomes. The prospect of achieving flexible dosing to fit the criteria of precision medicines is limited and highly challenging for most commonly produced oral SDFs such as tablets and capsules. This is mostly due to the very nature of such dosage forms and several processing factors involved during their large batch manufacturing processes. For this matter, liquids/suspensions have been considered more appropriate dosage forms for children from birth to 8 years old since they offer easier dose flexibility while eliminating undesired swallowing necessity of usual SDFs that many patients suffer from (EMA, 2006). However, liquid medicines face problems of their own such as precise adjustment of the correct dose, stability of the drug in the formulation, multiple administrations during the day for the lack of controlled-release profiles, not to mention the high

costs of handling, transportation and storage conditions of such bulky dosage forms. Moreover, the acceptability and palatability of the liquid dosage forms are lower than SDFs due to their usual bitter taste especially for children who have more distinct preferences for sweet tastes (Tanner et al., 2014). Altogether such negative factors related to liquid dosage forms make this option impractical as a concluding solution in pursuit of a universally accepted form of delivering flexible dosed formulations.

The only available option in the past to obtain the appropriate dose for a specific treatment was to split commercially available tablets and other solid dosage forms that come with fixed and limited API doses to the market (Rosenberg et al., 2002; Teng et al., 2002). However, even applying appropriate tablet splitting tools and procedures may compromise the accuracy of the final dose, the quality and integrity of the pre-designed dosage unit and the possibility of drug wastage. Shah et al. (2010) have expressed numerous potential concerns of such practice, including uneven drug content and the stability concerns of the drug in the remaining sections of the medicine. McDevitt et al. (1998) discovered that out of 1752 manually split tablets, a staggering 41.3% showed more than 10% deviation from the ideal weight while 12.4% had more than 20% deviation. Such undesirable variations may have devastating effects on a patient's health especially in case of drugs with a narrow therapeutic index (NTI) as well as heart and thyroid medicines in which the risk of under-dosing or over-dosing is more critical. The proper dose adjustment of such drugs becomes even more essential for patients who suffer from chronic diseases with persistent effects that require long-lasting medications.

It is worth mentioning that a new technology for tablet manufacturing was patented claiming to offer splitting options while providing consistent partial doses (Solomon and Kaplan, 2007). Also Laukamp et al. (2014) formulated a delivery method called 'solid dosage pen' involving carbamazepine loaded rods that were produced by hot-melt extrusion in which the dose flexibility could be achieved by slicing tablet-like pieces. However, naturally such claims, even when successfully accomplished, are limited to attain only a few doses from a larger unit and cannot possibly offer a convenient and practical range of dose flexibility.

In addition, regarding administration, studies have shown that patients with swallowing disorder, mental illness and dysphagia are amongst those who had suffered the most when consuming large oral dosage forms (Dixit and Puthli, 2009; Nilausen et al., 2011). There have been a number of publications stating that in general between 20% and up to 50% of all drug consumers experience swallowing discomfort when taking available SDFs (Brniak et al., 2015; Lau et al., 2015). McDevitt et al. (1998) additionally claimed that about 96.8% of the patients preferred commercially available lower dosed formulations while 77.2% were willing

to pay more for such products. To look more closely into the issue, Schiele et al. (2013) published a thorough study stating that out of 1051 participants, around 37.4% (N = 393) had faced swallowing difficulties regarding solid drugs in which younger and female patients were affected significantly more. The reasons for such difficulties were related to the size (74.6%), surface (70.5%), shape (43.5%), and flavor (22.1%) of the dosage forms.

Altogether, the abovementioned difficulties give rise to patient dissatisfaction and poor adherence to the treatment procedures. In this regard, the introduction of the precision medicine has fundamentally changed the medical practice to bring much-needed tailor-made medicinal products closer to reality with innovative delivery systems. The announcement of the Precision Medicine Initiative (PMI) in 2015 had a clear message that precision medicine had gained a universal momentum in its progress (The White House, 2015). According to researchers of Tufts center for the study of drug development (CSDD) in 2015, the United States Food and Drug Administration (FDA) had approved 137 drugs with pharmacogenomics information in their labeling in which 20% of all FDA approvals in year 2014 alone had belonged to the personalized medicines category (Tufts, 2015). Tufts (CSDD) press release further stated that biopharmaceutical companies were expected a 33% rise in investment on personalized medicine followed by 69% increase in medicines in development by 2020.

According to the FDA, 'the goal of personalized medicine is to streamline clinical decision making by distinguishing in advance those patients most likely to benefit from a given treatment from those who will incur cost and suffer side effects without gaining benefit'. Today, the worldwide wireless and computational advancements have paved the way for a more effective medical treatment and individual care including continuous monitoring of patients' response and health condition regarding their medication (FDA, 2013). The rapidly growing field of personalized medicine is the cornerstone in future research and development in the field of pharmaceutical sciences. Personalized medicine highlights a real medical need for the individuals to receive a customized treatment with a deeper understanding of their individual characteristics that governs the pharmacokinetics of the drug in their body. Furthermore, this concept aims to guarantee higher patient compliance and safety profile of the drug and the excipients which together will certainly result in a more successful therapeutic outcome.

2.2. Orodispersible films

'Orodispersible film' (ODF) is the preferred term for the European Medicines Agency (EMA) to describe thin, flexible, planar and stamp-sized polymeric films that are designed as single or multi-layer systems to be disintegrated rapidly when placed onto the saliva-wetted tongue without the need for drinking additional water

(Hoffmann et al., 2011). Such properties have made ODFs a promising approach for drug delivery with improved compliance and more convenient administration generally for pediatrics, geriatrics, psychiatrics and unconscious patients as well as those with Parkinson's disease, vomiting, swallowing disorder and dysphagia (Irfan et al., 2016). One of the most important advantages of such formulations is that when the drug is properly absorbed through the oral mucosa, it avoids the first-pass metabolism and enters directly into the blood stream resulting in greater bioavailability with an immediate onset of actions and pharmacological effects (Clarke et al., 2003; Zhang et al., 2002). Due to the novelty of this delivery method, ODFs have not been listed in any pharmacopeia yet. Therefore, there is a need for an official monograph to regulate their standard production, test procedures and analysis techniques (Preis, 2014). To be specific, so far no standard disintegration test with a definitive end point has been established for ODFs. This has led researchers to improvise and design different experiments that can be found in many recent publications (Garsuch and Breitkreutz, 2010; Low et al., 2015; Preis et al., 2014; Woertz et al., 2011). According to a published monograph (European Pharmacopoeia Commission, 2008) a 180s time interval was defined as the limit for disintegration of the *orodispersible tablets*. The 180s time interval is still used today also for disintegration time limit of the ODFs.

2.2.1. Manufacturing of orodispersible films

The first ODF in the market was introduced in 2001 by Pfizer as thin strips of breath-freshener Listerine® PocketPaks followed by the first over-the-counter (OTC) ODF containing an API (benzocaine) that was launched by InnoZen in 2003. Later, in 2010, the first prescribed ODF containing risperidone was made commercially available in the market (Hoffmann et al., 2011). In 2013, it was reported that most of the available ODFs were produced by the solvent casting technique (Genina et al., 2013b). The rest of ODFs are produced either by electrostatic spinning method or by hot melt extrusion method for modified release purposes (Palo, 2017).

In the solvent casting method, a powder mix of the drug, the film forming polymers, plasticizers and other excipients, if needed, is dissolved in aqueous or organic solvents and continuously stirred for a few hours. Later the obtained homogeneous viscous coating mass is uniformly spread out on top of an inert surface and is leveled to the desired thickness using a coating knife. The solvent is then allowed to dry so that a thin dry film remains. One substantial advantage of this approach is the manufacturing of the entire product using only one production line in which the dose adjustment is possible by simply cropping a certain size of the film (Preis, 2014). The great versatility of polymer-based orodispersible dosage forms has established their role as an appropriate and promising delivery platform for the demanding market (Borges et al., 2015).

However, regardless of the apparent simplicity of the solvent casting method in theory, it faces in reality potential challenges to guarantee a uniform thickness and the drug content uniformity in big scales where cropping a selective area may pose dose inaccuracy (Janssen et al., 2013).

Printing APIs onto placebo orodispersible films has been reported to be a smart solution to achieve dose precision for population-specific drug delivery systems which proposes yet another bid for application of the emerging inkjet printing for manufacturing of pharmaceutical products (Planchette et al., 2016; Scarpa et al., 2017). Janssen et al. (2013) have successfully printed low doses of rasagiline mesylate and tadalafil as the model drugs on placebo ODF carriers by the flexographic method in industrial scale and have compared the results with the common solvent casting technique. Usually the drug-free films are casted on top of an intermediate casting liner/surface (e.g. PET films) which is kept attached to the film to facilitate a flat and level printing job without rolling up, waviness or ripple effect on the film's surface during and after the printing procedure (Genina et al., 2013b).

2.2.2. Challenges and shortcomings

ODFs need to have a fast disintegration time while having a certain mechanical stability to ensure a robust and practical manufacturing and packaging for easier handling, storage and administration (Peh and Wong, 1999). The challenge is to fulfill such requirements considering the fact that there is an inverse relationship between stronger mechanical properties and the disintegration time of a thin film. However, a very fast disintegration time is not optimal since there may not be enough time for proper drug absorption in the mouth. Acceptable bioavailability and safety of the excipients for pediatrics and especially neonates and infants with enzymatic immaturity can further complicate the choice of the excipients for such patients (Breitkreutz and Boos, 2007). In addition, due to the nature of this delivery system, the drug load is limited. Therefore, the application of ODFs is mostly restricted to low doses of highly potent drugs (Hoffmann et al., 2011). Most importantly, since the APIs dissolve in the saliva, pleasant taste and organoleptic properties would play a major role in palatability and compliance particularly for pediatric patients. Taste masking methods could further limit the drug load and in case of extremely bitter APIs it could even be impossible to accomplish. The taste attributes of the ODFs remain the main drawback for this delivery system to date which is discussed extensively by Preis (2014) and Walsh et al. (2014).

2.3. Inkjet printing technology

The need for ever-growing customized products has persuaded pharmaceutical companies of all magnitudes to consider a shift from the paradigm of large-scale batch production, which is both highly labor and capital-intensive, towards more

decentralized small-scale manufacturing strategies. The small-batch production of patient-specific pharmaceutical products in a continuous process design is the defining strategy that can keep the companies at the forefront of the business competition in an emerging era of personalized medicine.

The advancement in design, robustness and flexibility of non-contact industrial inkjet printers along with the diversity and simplicity in digital design of the formulations can make way for a paradigm shift in pharmaceutical manufacturing processes (Melendez et al., 2008; Scoutaris et al., 2016). The research and development related to applications of inkjet printing technology as a low-cost, eco-friendly, compact and highly reliable method for small batch production of oral SDFs have been substantially increasing during the past decade (Buanz et al., 2011; Janssen et al., 2013; Sandler et al., 2011).

Inkjet printing includes a wide range of high speed technologies that are capable of direct deposition of thousands of droplets onto specifically defined locations on various porous substrates through microscopic nozzles in a digitally-controlled environment. In this regard, inkjet printing technology can be implemented for rapid manufacturing of extremely uniform, precise and low doses of a variety of drugs, with more focus on poorly water soluble and narrow therapeutic index drugs, in single or multi-drug delivery system for personalized therapy (Alomari et al., 2015; Preis et al., 2015; Raijada et al., 2013). Hirshfield et al. (2014) used inkjet printing technology to construct a small scale, automated and controlled manufacturing method called dropwise additive manufacturing of pharmaceutical products (DAMPP) for deposition of both the API and the polymer excipient directly onto edible substrates. In this sense, DAMPP could provide a practical alternative to traditional large-scale batch manufacturing processes with their many limitations in terms of process control and automation.

Inkjet printing technology also provides delivery solutions for large and complex biological drugs such as peptides and proteins (Montenegro-Nicolini et al., 2017). The formulation of biological drugs usually faces more difficulties due to their large molecular size, selection of appropriate excipient, poor membrane permeability and instability in enzymatic solutions (Kolakovic, 2013a). Such drugs are also prone to first-pass metabolism and require specific and targeted delivery in small doses (Ross et al., 2015). In addition, nanosuspensions containing poorly water soluble drugs in the form of conventional crystalline nanodrugs together with stabilizing emulsifying agents or in the form of 'amorphous drug nanoplex' have also been printed for personalized therapy (Cheow et al., 2015; Pardeike et al., 2011). The technology further offers opportunities to produce oral and non-oral (topical, implants, etc.) drug formulations mostly for immediate release (Palo et al., 2017) and less considerably for modified release purposes (Gu et al., 2012; Preis et al., 2015; Uddin

et al., 2015). The controlled-release formulations can be prepared either by direct printing of the drug-polymer ink solution or by polymer coating of already inkjet printed formulations containing the API (Genina et al., 2012; Scoutaris et al., 2011). The rate of the drug release can also be controlled by selecting different carrier geometry patterns as crucial design parameters affecting the interaction of the delivery system with the tissues mainly due to the changes in the surface area (Lee et al., 2012).

In conclusion, from the industrial point of view, inkjet printing further offers an inherently scalable and continuous process with high reproducibility, improvement in product quality and minimal waste and contamination. Additionally, the potential to eliminate many middle steps of the conventional solid dosage production and a subsequent drastic reduction in the energy consumption, further help to optimize the cost and efficacy of the drug delivery systems that are produced by inkjet printing technology.

2.3.1. Inkjet printing classifications

Inkjet technology is classified into two categories, namely continuous inkjet (CIJ) printing and drop-on-demand (DoD) printing that are distinguished by the physical process that is involved in generation of the droplets (Derby, 2010). The underlying principle in CIJ printing is breaking up a continuous stream of fluid into droplets at regular intervals by perturbation. A portion of the generated droplets are then deflected after leaving the nozzle according to the print pattern either by high voltage electrical fields, airflow or sometimes thermal steering. This portion of the droplets continue their flight path onto the surface of the substrate at angles proportional to the degree of deflection while the undeflected portion is collected by a gutter and fed-back into the ink circulation system. Such printing principle makes CIJ printing a high-speed process. However, the print resolution is compromised.

On the other hand, in the DoD method the droplets are formed impulsively and are ejected only when required. The activating signal is usually an electric signal that is applied close to the orifice cavities of the nozzles. DoD printing has been utilized more widely in pharmaceutical research applications since it offers more control over the deposition of the droplets and the fact that only small volumes of ink solutions are required for the printing job as opposed to a large recirculating volume that is needed for CIJ printing.

2.3.2. Thermal and piezoelectric inkjet printing

Drop-on-demand technologies are mainly divided into two categories of thermal inkjet printing and piezoelectric inkjet printing according to the technique that is employed to eject the droplets. The sophisticated and immaculate design of the thermal inkjet printing technology is found in every day consumer desktop printers

which are quite affordable and readily available. In thermal inkjet printing the image signal is transmitted by a highly accurate electric current network of up to 400 miniaturized elements, each in contact with the ink next to a nozzle on the silicon printhead. According to the digital print signal, a pulsed supply of electric charge heats up the elements to up to 300 ˚C for a very short period of 2 to 10 µs (Hölzl et al., 2016; Melendez et al., 2008). The rapid rise of temperature causes localized evaporation of the ink followed by formation of an ink bubble. The expanding bubble forces a drop out of the nozzle orifice. When the signal ends, the bubble collapses and the resulting negative pressure fires the drop out while a new drop is simultaneously replaced into the nozzle chamber. The drops in the volume range of 2-180 pl are usually ejected in the frequency range of 5 to 10 kHz out of hundreds of nozzles in the diameter range of 10-50 µm and reaching the speed of up to 10 m/s (Melendez et al., 2008). The spatial location of the landing droplets is also digitally controlled by a motor which is highly aligned with the image signal in pixel-level precision (Kolakovic, 2013b; Le, 1998).

In piezoelectric inkjet printing, the image signal is produced by voltage tuning of a piezo-element in contact with the ink. The piezoelectric element that produces a deformation mode causes a pressure wave which regulates the flow of the drops out of the nozzles by mechanical displacement (Le, 1998). A wider variety of liquids with higher drop frequency can be printed by piezoelectric technique as compared to thermal inkjet printing while the application of relatively cheaper thermal inkjet printers is limited to mainly aqueous solutions with suitable vaporizing properties (Kolakovic, 2013b).

Modified consumer desktop thermal inkjet printers (Buanz et al., 2011; Genina et al., 2013b) and Dimatix Materials piezoelectric inkjet Printers (Genina et al., 2013a) have been used more frequently due to their high availability and reliable performance, in addition to low-cost and compact design with disposable ink tanks. Such characteristics make these printers great candidates to be used in a pharmacy or hospital settings for late-stage tailored delivery systems. Planchette et al. (2016) used both piezoelectric and solenoid valve-based inkjet printing techniques, that adjusts the nozzle opening by the electromagnetic force from an energized solenoid coil, to print two different inks solutions on various medical-grade oral films. In addition, they successfully coated a non-porous substrate with a hydrophilic polymer in polyethylene glycol (PEG) prior to printing to homogenously distribute the poorly water soluble API on the coating layer and to avoid crystallization of the drug in addition to taste-masking purposes. Finally, in a classic and thorough study by Wickstrom et al. (2015) piezoelectric inkjet printed systems containing poorly water soluble drug indomethacin with flexible doses was produced on porous substrates. They further studied the solid-state properties of the formulations, the

printability of various inks regarding their rheological properties, the influence of the excipients and finally the improvements in the dissolution rate of the amorphous API in the printed formulations.

2.3.2.1. Printing parameters for piezoelectric inkjet printing

Careful adjustment and optimization of printing parameters and particle size in a specific ink solution further guarantees a continuous and uniform automated printing job. The main parameter for a piezoelectric inkjet printer is an electric waveform consisting of the voltage and the pulse shape that is applied to the piezoelectric element. The electric waveform dictates the shape, size and proper formation of ejected droplets and in short, the printability of the ink (Mogalicherla et al., 2014). McKinley and Renardy (2011) discussed extensively about printability of ink formulations based on two major parameters of viscosity and surface tension along with the density of the ink that altogether influence the dimensionless *Z-value* as the criterion for printability. Hutchings and Martin (2012) specified a typical viscosity range from 1 to 20 mPa.s and a surface tension range from 25 to 60 mN/m for available inkjet printers. However, such specifications are not absolute and have also been reported with variations such as 2-30 mPa.s and 25-50 mN/m (Daly et al., 2015). Similarly, a Z-value in the range of 1 to 14 has been reported to be optimal for printing (Derby, 2010). In order to avoid clogging of the nozzles and guarantee a smooth and continuous printing job, the particle size of the drug in the ink solution should also be taken into account according to the nozzle diameter. For a printable ink containing API particles, volume distribution value (d_v90), which is the value that 90% of the particles have smaller diameter than this value, should be less than 2% of the nozzle diameter (Kuscer et al., 2012).

2.3.3. Flexographic inkjet printing

Apart from the classic inkjet printing techniques, there is also flexographic printing which is a modern version of letterpress printing method with the possibility to print a diverse range of aqueous, polymer-based solutions and nanosuspensions onto a large variety of flexible substrates and surfaces (e.g. plastic, foil, paper, etc.). Inks with viscosity range from 50 to 500 mPa.s and surface tension between 25 and 45 mN/m can normally be printed using the flexographic method (Ihalainen et al., 2015). In this sense, the flexographic method provides certain possibilities for printing high molecular weight species such as proteins and biomolecules in highly concentrated inks. Flexographic printing can also be used to print highly viscous polymeric solutions for coating purposes to achieve modified release profiles or taste masking with or without the inclusion of the API. However, the printing resolution and the control over spatial deposition of the ink are compromised. Thus, the pharmaceutical application of this printing method has not been yet intensely investigated.

Flexographic printing is a rotary printing process in roll-to-roll fashion that is used primarily for packaging and labeling of products. In this method, a rotating 'fountain cylinder' in contact with the ink tray picks up the ink and transfers it to the 'anilox cylinder' which has cell patterns on its surface. The ink on the anilox cylinder is leveled with a doctor blade, so that a certain and uniform amount of ink is fed onto the 'plate cylinder' that has raised (relief) patterns attached on its outer surface as the image to be printed. This raised pattern is usually made of a low-cost flexible polymer which is simply attached around the plate cylinder by two-way adhesive tape. Finally, an 'impression cylinder' is used to apply a force, usually between 50 to 200 N, to the ink covered relief pattern plate with the substrate sandwiched in between, so that the pattern is imprinted onto the substrate.

2.4. Analytical methods for quality control of printed medicine

It is understood that quality control of the pharmaceutical products has the utmost importance in regards to the safety, the integrity of the dose and the overall therapeutic effects of the medicinal products. Quality control methods also provide information regarding the degradation process of the drug in formulation that ultimately defines the shelf life of the product.

Process analytical technology (PAT) is defined as a system to design, analyze and control pharmaceutical manufacturing processes through well-timed measurements of Critical Process Parameters (CPP) and Critical Quality Attributes (CQA) of raw and in-process materials as part of a Quality by Design (QbD) approach to guarantee the desired final quality of the products. In 2004, FDA initiated PAT as a guidance to encourage and promote voluntary adoption of innovative manufacturing technologies to improve the quality assurance and the efficacy of the drug development (FDA, 2004). This non-binding regulatory framework aimed to gain deeper insights into the factors that influence the production process parameters, particularly in technologically complex procedures that oblige more strict protocols (Korasa et al., 2016).

In this regard, it was envisioned that at/in/on-line integration of miniaturized and non-invasive measuring probes together with the application of concrete data analysis tools, if needed, could provide greater control over the state of the pharmaceutical materials and processes during the production.

FDA also have allowed continuous processing of pharmaceutical products according to the QbD principle in which in-depth control of raw materials and process parameters ensures the high quality manufacturing of the final products (Linden, 2012). FDA underlined that the quality must be built into the product by designing a robust formulation and manufacturing procedures rather than increased testing of products and processes (Yu et al., 2014). The industrial inkjet printers that are already available in the market provide high accuracy and quality of the printing

process. Therefore, the QbD principle of the printed products that are manufactured by such printers can be fulfilled by careful selection of the ink solution with specific rheological properties together with smart combination of the API and medical grade carrier substrates that are suitable for the printer in use. The final quality of the inkjet printed formulation is highly dependent on the precision of the engineering design of the employed machinery, printability of the ink solution and the physicochemical properties of the API both in the liquid state in the ink solution before and during printing and the solid-state within the substrate matrices after printing.

The main problem in the way of inkjet printing technology becoming a genuine and viable method for continuous manufacturing of solid dosage forms is the lack of rapid, robust, reliable and non-destructive analytical techniques for real-time quality control of the printed formulations (Edinger et al., 2017). The necessity of the alternative quality control devices for printed formulations which was addressed earlier by Raijada et al. (2013), still stands today.

This research was mainly focused on the feasibility of various quality control methods to monitor the drug content and the drug release from the printed formulations. Such quality control techniques offer a significant reduction in procedure time of the conventional quality control methods which are lengthily, tedious and labor-intensive. In this regard, this thesis aims to provide the necessary initials to make way for the much-needed shift in the quality control approaches towards more improved and possibly automated analytical techniques in search of making inkjet printing a viable, realistic and continuous process of manufacturing orodispersible formulations for personalized therapy.

For this purpose, the application of potentiometry, hyperspectral NIR imaging, colorimetry and NIR spectroscopy was proposed to create a platform for fast, easy to use, reliable and non-invasive alternative analytical techniques for inkjet printed formulations. The compact and robust design of the small-scale probes such as the ion-selective electrodes (ISEs) as well as the non-invasive nature of the handheld colorimeter and the NIR spectroscopic device offer an indispensable factor for in/on-line adoption in the production line at the envisaged point of care. In addition, the fast and non-intrusive NIR hyperspectral imaging technique that is designed for integration in the continuous processes further allows in-process monitoring of the uniformity of the API distribution and the overall consistency of the final products. The application of such advanced process control methods, when properly determined by the regulatory authorities, will provide alternative means for a closer monitoring of the quality aspects of the printed formulations in real time.

A summary of the literature review on the employed analytical techniques is presented below.

2.4.1 Potentiometry

Potentiometry is a well-known analytical technique with a long history in measuring the electrical potential difference or electromotive force (EMF) between a reference and a working/indicating sensor in a sample solution. Ion-selective electrodes (ISEs) are the most frequently used electrochemical sensors that facilitate the conditions for an ionic exchange process in which the potential build-up at the boundary of the membrane/solution can be measured and correlated to the concentration of the target ion in the solution. ISEs respond selectively by design to a particular electroactive species in a solution. Such sensors are capable of correlating the electric signals to the chemical information and vice versa by means of a conditioned membrane that is connected to an ion-to-electron transducer. The generated boundary potential is measured against the potential of a stable reference electrode and it can be used for quantitative analysis of the target ion in real time. Nernst equation correlates the electrical potential difference between the two electrodes to the activity of the ion that initiates such phenomenon:

$$\Delta E = \frac{RT}{\chi F} \ln (\alpha_m/\alpha_i) \text{ (aq)}, \quad (1)$$

where ΔE is the potential difference measured between the working and the reference electrodes (V), R is the universal gas constant (8.314 J/mol. K), T is the absolute temperature in (K), χ is an integer representing the charge of the target ion, F is faraday constant (96,485.3 C/mol), α_m is the activity of the target ion in the membrane and α_i is the activity of the target ion in the analyte solution. Necessary assumptions are made in order to make a simpler and more practical version of equation (1). For example, the negligible potential change in the reference electrode is ignored and the activity of the target ion is replaced by its concentration assuming an ideal case of a clear dilute solution. Therefore, substitution of the constant values into equation (1) results in:

$$\Delta E \text{ (mV)} = 59.2/\chi \log (C_m/C_i) \text{ (Mol)}, \quad (2)$$

where C_m is the concentration of the target ion in the membrane and C_i is the concentration of the target ion in the analyte solution. When plotting the potential difference (ΔE) against the logarithm of the ion concentration (log C), a linear section representing 'the Nernstian behavior' of the electrodes with the slope of $59.2/\chi$ mV at 25° C should represent the ideal value for the electrodes. The shape of 'ΔE vs. log C' plot starts to deviate from a straight line (to more like an 'S' shape figure) at both ends of the curve. In order to accurately detect both the upper and the lower detection limits of the electrodes as recommended by International Union of Pure and Applied Chemistry (IUPAC) (Buck and Lindner, 1994), a tangent line from each deviated end is intersected with the linear section. The concentration

values at the points of intersect are considered as upper and lower detection limit for the electrodes.

Apart from numerous applications of ISEs in various fields of science, they have been used broadly in the pharmaceutical field for quantitative analysis of many APIs in formulations in the past couple of decades (Aboul-Enein and Sun, 2000; Giahi et al., 2010; Khalil and Borham, 1999; Salem et al., 2003; Shamsipur et al., 2002). The conventional ISEs that are designed with an internal filling solution containing the ion of interest that is connected to the selective membrane, impose problems regarding their working conditions, maintenance and lifetime. In the past few decades, several breakthroughs have made a massive impact on revitalization of the ISE applications. Introduction of all solid-contact ion-selective electrodes (SC-ISEs), the progress in deeper understanding of the ion flux through the membrane and the influence of interfering ions and most importantly the major improvements in the lower detection limits have made great advancements in this field (Sundfors, 2010). Today, the SC-ISEs offer numerous advantages such as simple, portable and low-cost design, easy maintenance, long durability, appropriately low detection limit, fast response time, strong selectivity for a wide range of APIs in solutions or various charged electrolytes in the blood and other body fluids, high tolerance in a wide pH range, insensitivity towards many common excipients and the possibility to function in colored and cloudy solutions.

Construction of SC-ISEs involves casting of the ion-selective membrane directly on the surface of a solid electric conductor which eliminates the internal liquid filling and provides simpler design, easier maintenance and more mechanical flexibility and robustness. The membrane is the heart of the ISE which is usually made of a highly viscous and lipophilic polymeric solution preferably with low water uptake and practically fixed composition of carefully selected constituents. The polymeric membrane is typically consisting of 66w% plasticizer, 33w% high-molecular weight PVC and 1w% of *ionophore* (Bakker et al., 1997). The mix of the components is usually dissolved in an organic solvent with a low boiling point such as tetrahydrofuran to achieve a *membrane cocktail* for casting. The key constituent for the selectivity of the membrane is the ionophore substance that enables reversible binding to the target ion as the driving force behind the functionality of the electrodes. Bühlmann et al. (1998) published a comprehensive review on all classes of readily available ionophores that had been used for many target ions. It must be noted that in many cases the ionophore substance can be entirely replaced or used together with a lipophilic complexing agent (salt) that provides the ion-exchange properties to the membrane as the prerequisite for the Nernstian behavior of the electrodes (Mattinen et al., 2009; Sundfors, 2010). The two most common lipophilic salts that are used in the membrane are potassium tetrakis[3,5-bis(trifluoromethyl)phenyl]borate (KTFPB) and potassium tetrakis(4-

chlorophenyl) borate (KTpClPB) which are for anion-selective membranes and cation-selective membranes, respectively.

Apart from the constituent of the membrane, the ion-to-electron transducer within the SC-ISEs structure is also important in the overall performance of the electrodes. In the past, conducting polymers have been widely used as ion-to-electron transducers (Bobacka, 1999; Bobacka et al., 2008). However, more recently, new classes of materials such as microporous carbon (Lai et al., 2007), carbon nanotubes (Rius-Ruiz et al., 2011) and most importantly carbon cloth have been implemented for such purpose. Mattinen et al. (2011) performed a comparative study on ion-to-electron transduction process and concluded that carbon cloth offers more qualities than conductive polymers or bare glassy carbon while providing even more mechanical flexibility and robustness to the manufactured electrodes. The good qualities of the carbon cloth were attributed to its inherently high specific surface area, large double-layer capacitance and low impedance at the membrane interface followed by a good potential stability.

2.4.1.1 The working principle of the ISEs

In the membrane, the lipophilic salt dissociates into two ions, usually a lipophilic ion and a smaller hydrophilic ion. The hydrophilic ions (e.g. K^+, Ca^{2+}, etc.) must have the same charge as the target ions which are actually the ionized API molecules. The lipophilic ions in the membrane which are stationed in the membrane with the opposite charge as the target ions are called *ionic sites*. These ionic sites are the destination for the flux of target ions to the membrane. The more lipophilic target ions have a tendency to substitute the small hydrophilic ions at the ionic sites. The electrodes must be conditioned in a solution containing the target ion for several days prior to measurements, so that the activity of the migrated target ion in the membrane reaches equilibrium. This provides the necessary factor for the electrodes to be able to detect any changes in ionic concentration when introduced to solutions of unknown concentrations (Bakker et al., 1997). When electrodes are submerged into the analyte solution with a different ion concentration as the conditioning solution/electrode membrane, a charge separation occurs at the interface of the membrane and the bulk of the analyte solution. This charge separation causes a phase-boundary potential which is ultimately measured. The degree of lipophilicity of the target ions governs the interference of the counterions and dictates the lifetime of the electrodes. The inevitable leaching of the complexing agent/ionophore into the surrounding aqueous solutions results in depletion of the membrane from its active component(s) which subsequently exhibits an undesirable potential drift away from the Nernstian behavior (Bakker et al., 1997).

2.4.2 Colorimetry

Color is the primary parameter that highly influences the consumer's final opinion and overall acceptance of any edible products. Analytical techniques that use colorimetric measurements in the visible part of the electromagnetic spectrum have been explored extensively in the past for quality control of the food products (Ansorena et al., 1997; Calvo et al., 2001; Kays, 1999; Meléndez-Martínez et al., 2003). Since color is not an intrinsic property of an object, the changes in illumination conditions (e.g. light intensity) together with the angles of illumination and viewing affect the color evaluation (Meléndez-Martínez et al., 2005). Even though human vision is highly robust regarding true perception of color, the visual color examination is inherently subjected to variation from observer to observer and clearly is not practical for large-scale color measurements (Zhou et al., 2011). Therefore, in order to conduct an objective analysis, proper color measuring instruments have been introduced along with defined color spaces in which each color corresponds to certain color components or tristimulus values (Trussell et al., 2005). Di Wu and Sun (2013) described the color space as 'mathematical representation for associating tristimulus values with each color.' Three different color spaces, namely RGB (red, green, and black), CMYK (cyan, magneta, yellow, and key) and CIELAB have been defined to describe color as a number in 3D space.

CIELAB color space was established in 1976 by Commission International d'Eclairage (CIE) and has been adopted as an international standard for color measurements by many instruments ever since. CIELAB is a perceptually uniform color space which means that 'the Euclidean distance between two different colors corresponds approximately to the color difference perceived by the human eye'. Therefore, it estimates/mimics the human color perception and sensitivity with high accuracy (Zhou et al., 2011). When using a spectral sensitive tristimulus colorimeter in CIELAB color space, the colors are described by three numerical values (vectors) of L^*, a^* and b^* in different recommended illuminant/observer settings (Korifi et al., 2013). L^* is the intensity component of the color ranging from the darkest black to brightest white (0–100) and parameters a^* and b^* are the other two chromatic components that represent the shift from green to red and from blue to yellow in a range of -100 to +100, respectively. Finally, the color difference parameter (ΔE^*ab) is expressed in Cartesian coordinates according to:

$$\Delta E^*_{ab} = \sqrt{(L^*_1 - L^*_0)^2 + (a^*_1 - a^*_0)^2 + (b^*_1 - b^*_0)^2}, \qquad (3)$$

where (L^*_1; a^*_1; b^*_1) are *the measure* coordinates and (L^*_0; a^*_0; b^*_0) are *the reference* coordinates.

In this manner, using the reflective light mode from the surface of the samples in the entire visible spectrum, a complex color as a quality factor can be expressed in numerical values for objective quantitative analysis.

The application of colorimetric techniques in quality control of the pharmaceutical products has been limited, even though low-cost and easy to use colorimetric instrumentations have been readily available (Zhou et al., 2011). Hetrick et al. (2013) used a colorimetric technique to assess the physical appearance and the color coating stability of the pharmaceutical dosage forms in accelerated conditions to replace the current subjective man-based visual tests for such purposes. Wickstrom et al. (2017) further demonstrated the applicability of the same colorimetric device in this thesis for estimation of vitamin B_1, B_2, B_3, and B_6 amounts in orodispersible formulations. They reported that after a certain number of printed layers, the color saturation set the upper detection limit for the device. Also, Al Hagbani et al. (2017) used a colorimetry in CIELAB color space to identify the imitator products including many forms of sildenafil tablets from the innovator Viagra® tablets. The application of such technique can avoid major public health concerns in developing countries with poor regulatory practice and dominant counterfeiting issues.

Since most APIs are colorless, both in powder form and in various aqueous or organic solutions, an assumption was made for addition of a coloring agent to the ink formulation so that the color difference measurement could be feasible. The goal was to investigate if a meaningful correlation between the colorimetric coefficients and the escalating number of printed layers could be achieved. In this manner, the drug content could be indirectly estimated by the applied colorimetric technique since the number of printed layers has been consistently proved to be linearly proportional to the drug amount in each formulation.

2.4.3 Vibrational Spectroscopy

The electromagnetic spectrum is divided into various sections extending from one side to the far most regions of ultraviolet and from the other side to the far most regions of infrared **(Figure 2)**.

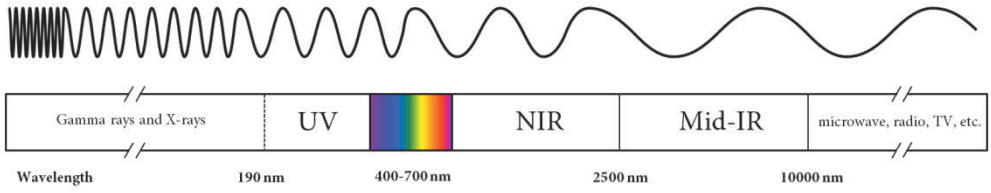

Figure 2. *The electromagnetic spectrum in logarithmic scale.*

Matter can absorb, reflect, transmit or scatter light when exposed to the electromagnetic radiation. The underlying physical concept of spectroscopy is the measurement of the interactions of the inherent electromagnetic field of the sample

with the electromagnetic radiation that is subjected to the sample. In classical physics, this interaction occurs only if the frequency of the electromagnetic radiation matches the frequency of various vibrational modes in atomic bonds within the molecules under study (Raghavachari, 2001). Vibrational spectroscopy is the study of specific frequencies of light that generate vibrational movements in form of symmetric or asymmetric periodic motions such as stretching and bending in chemical bonds which alter the energy levels of a substance for a short time.

Highly versatile vibrational spectroscopic techniques including mid-infrared (mid-IR), near-infrared (NIR) spectroscopy and imaging together with Raman spectroscopy and imaging provide fast and nondestructive physicochemical analysis of pharmaceutical products with little to no sample pretreatment requirements. Each spectroscopic technique functions in a specific frequency range of the electromagnetic spectrum which dictates the energy level that is radiated to and collected from the samples. Lights of specific wavelengths are absorbed or scattered in different regions of electromagnetic spectrum according to molecular bonds within the sample. The spectroscopic measurement can be used to both identify the chemical structure and to quantify the composition of various raw and in formulation substances.

2.4.3.1. NIR spectroscopy

According to The American Society of Testing and Materials (ASTM), the NIR region of the electromagnetic spectrum includes wavelength range of 780–2526 nm which is corresponding to the wave number range of 12820–3959 cm^{-1}. The mid-IR region extends beyond the NIR region from 4000–400 cm^{-1} (2.5–25 μm). The most prominent absorption bands (peaks) in the NIR region are related to overtones and combination of fundamental vibrations of hydrogen bonds such as C–H, N–H, O–H, etc. These absorption bands which are derived from fundamentals in the mid-IR region are normally broad and overlapping where the stronger bands may obscure neighboring weaker bands. For this reason, the NIR variables (wavelengths) are often partially or completely collinear and the meaningful information is hidden in their correlation pattern rather than in individual and selective absorption band signals in mid-IR region (Eriksson et al., 2013). Therefore, due to the multivariate nature of the data, it is highly unlikely to correctly associate the peaks in the spectra to known physical or chemical properties of the samples (Stenlund et al., 2009). However, the very existence of peaks in the spectra indicates the relevant chemical information and their absence are considered as irrelevant information or noise.

NIR spectroscopy has been used extensively in the pharmaceutical field as a PAT tool for identification and quantification of raw, intermediate and finished pharmaceuticals as well as for monitoring of such manufacturing processes. In particular, NIR spectroscopy has been employed to study the API content (Järvinen

et al., 2013; Martínez et al., 2013), moisture content (Chablani et al., 2011; Mainali et al., 2014), quantification of excipients (Karande et al., 2010), the quality of film coating (Gendre et al., 2011; Korasa et al., 2016), monitoring various steps of production process (Blanco et al., 2010) and other applications.

The advancements in the field of fiber optics in NIR devices, the computing powers of modern instruments and the enhanced chemometric software with user friendly interface and useful graphical tools have been the core to higher acceptance of NIR spectroscopy in raw material testing, process monitoring and quality control in industrial scales (Reich, 2005). However, restrictive specifications and requirements of the pharmaceutical regulatory agencies regarding the quality control methods and the overall safety of the medicinal products have been the reasons behind the slow adoption of NIR spectroscopic techniques in the pharmaceutical industry. Such strict regulations are mainly due to the need for additional mathematical data analysis for examination and interpretation of the NIR spectra.

Considering the instrumentation, generally the premiere source of radiation for NIR spectrometers is tungsten halogen lamps which are small, inexpensive, stable, sturdy and readily available. Detector types include silicon, lead sulfide (PbS) and indium gallium arsenide (InGaAs). The silicon detectors are fast, small, inexpensive, and highly sensitive mostly in higher overtone regions (750-1100 nm). PbS detectors are also sensitive with good signal-to-noise ratio in a wider NIR region (1100-2500 nm), but they function relatively slower with more difficulty in production and operation. InGaAs detectors have been implemented more recently in larger fields of applications with combined positive properties of silicon and PbS detectors; however, they are much more expensive in comparison (Raghavachari, 2001).

The NIR spectra are usually collected from the surface of the solid dosage forms. This can be problematic for the analysis of the tablets as any given cross section of a tablet cannot possibly represent the true amount of API/excipient blend ratio in the entire dosage form. Moreover, it is evident that the assay of coated tablets is challenging since the spectral information arising from the coating polymers strongly affect the data (Reich, 2005). In this regard, the thin and planar surface of an orodispersible film offers a great advantage for NIR spectroscopy and imaging techniques for analysis of such dosage form in its entirety.

2.4.3.2. Hyperspectral NIR imaging technique

The application of hyperspectral NIR imaging in pharmaceutical research and development has emerged very recently as a complimentary method to NIR spectroscopy. This technique offers the possibility to create concentration distribution maps of the constituents at the pixel level so that the overall uniformity of the API and the excipients in the final product can also be assessed (Amigo and Ravn, 2009). The idea of complete inspection of the microstructure of the

formulations in a non-invasive fashion opens up a new quality control platform which allows compositional analysis to be integrated in form of convenient and easy to interpret color coded computer generated images with little to no sample preparation. Once again the enormous amount of hyperspectral data that are collected within a short time frame calls for multivariate methods to decode pixel-to-pixel qualitative, quantitative and spatial information.

Alexandrino and Poppi (2013) claimed to have used NIR chemical imaging and relevant chemometrics for the first time to create quantitative compositional distribution maps for both the drug and the excipients in thin film formulations. Zidan et al. (2010) used NIR spectroscopy and imaging techniques to evaluate the contents of a model protein in nanoparticles and to distinguish between 12 different formulations. Pavurala et al. (2017) used NIR hyperspectral imaging to model and predict the dry coat thickness uniformity of transdermal patches and to detect and identify thickness variations and practical defects related to non-uniform regions such as the presence of air bubbles. Franca et al. (2016) was able to monitor the degradation pattern of captopril into captopril disulfide in different layers of the tablets along with the detection of anomalies consistent with the manufacturing in addition to being able to reversely predict the manufacture date of the tablets within 120 days. Ely and Carvajal (2011) used NIR hyperspectral imaging to quantify the scale of segregation, as a quality factor to compare agglomeration of mixtures, in compact powder blends of low dose tolmetin (0-10% w/w) and lactose anhydrous as the diluent. They reported that a mixture containing 5% (w/w) tolmetin showed the best results before the spectral signals from higher percentage of the drug dominated the images. In a comprehensive and important review by Amigo (2010) a detailed description of advantages as well as practical issues regarding the application of hyperspectral imaging and data analysis approaches was published. Amigo (2010) stated that the pixel size should be selected according to the particle size of the API in the formulation, especially in lower doses so that the API signal remains significant. In addition, parameters such as the spatial resolution of the device, irregularities in the surface of the samples and the homogeneity of the drug on the surface which might not properly represent the entire formulation should be considered.

2.4.3.2.1. NIR hyperspectral imaging configurations

There are two main methodologies to conduct hyperspectral imaging in order to obtain a three-dimensional (X × Y × λ) 'hyperspectral data cube'; push-broom imaging and tunable spectral filter methods **(Figure 3)**. In push-broom imaging, the entire range of the NIR wavelengths (λ) is collected simultaneously one line at a time (in X direction) as the sample moves on a trail underneath the NIR camera (in Y direction) so that the final spectral image is built through line by line spectral

sweeping of the samples. In tunable spectral filter method, the entire sample area (X × Y) is illuminated throughout the measurement so that the spectral signal for each individual wavelength is collected from the entire pixels in view to build the final spectral image.

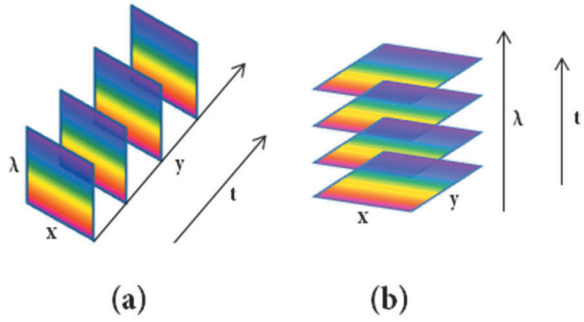

Figure 3. *The main hyperspectral imaging methods. (a) Push-broom and (b) tunable spectral filter.*

In short, in push-broom imaging *spatial lines* are scanned over time while in tunable spectral filter *the wavelength* is scanned over time. Push-broom imaging has more advantages due to simpler illumination standards, higher imaging speed and mainly because of the significant reduction in the heat load exerted to the sample as a result of line illumination of a moving sample that allows less damaging exposure time to the NIR light. More importantly, the push-broom method is designed for online process monitoring of products where samples are usually in a continuous movement along the production line.

2.4.4 Chemometric analysis

2.4.4.1 Data pretreatments

Data pretreatment is usually performed prior to multivariate modeling to reshape the data with least possible signal distortion, remove the irrelevant variations and artifacts such as background effect e.g. from substrate, eliminate nonlinearities and skewed distribution of single variables and finally to remove the baseline shift and slope for proper data analysis. However, using such mathematical modifications always leaves the risk of unintentional removal of some spectral features that may contain useful information. Therefore, it is important to select appropriate treatment methods according to the type and nature of the data in hand. One must consider that preprocessing cannot compensate for poor data quality, but often can make a good model better. Pretreatment techniques are mainly either scatter correction methods such as multiplicative scatter correction (MSC) and standard normal variate (SNV) or derivation methods such as Savitzky-Golay (SG) or Norris-

Williams. Such techniques and various similar methods have been discussed extensively in the literature (Barnes et al., 1989; Rinnan et al., 2009; Savitzky and Golay, 1964). In this thesis, the focus was on SNV scatter correction and Savitzky-Golay smoothing and derivation techniques.

2.4.4.1.1. Standard normal variate and Savitzky-Golay techniques

SNV is the second most used scatter correction technique after MSC. It works by subtracting the mean spectrum from the original spectrum and dividing it by standard deviation as the scaling factor for removing the artifacts or the scatter effect in the data. The signal-correction principle for SNV is the same as MSC, but the signal correction is not reference based. Thus, each spectrum is processed alone with no regard to the remaining of the data set. The minor differences between the two methods are related to a simple rotation and offset correction (Rinnan et al., 2009).

SG smoothing technique scans through the spectra in a polynomial form and approximates the smoothing and derivation for each variable separately in a single step (Vivó-Truyols and Schoenmakers, 2006). There are three parameters that should be decided before SG smoothing. The number of smoothing points which is a window of odd number of adjacent variables, so the point to be smoothed always situated in the center, the polynomial order of the best fit smoothing function and the degree of derivation. Normally a first derivative with 5-9 points or a second derivative with 7-11 points are used together with a 2^{nd} or 3^{rd} degree polynomial order as the common practice in NIR community. As the degree of derivation increases, the signal-to-noise ratio decreases. Thus, if a 3^{rd} degree derivative approach is selected, it is only logical to select a wider window of smoothing points (e.g. 15 points) and the lowest polynomial order. This can increase the signal-to-noise ratio and the resolution of the overlapping bands as well as in between the spectra in the search to find the optimal smoothness (Reich, 2005).

2.4.4.2 NIR data analysis

After a successful smoothing and scatter correction, there is a need for reduction of variables so that the data variability could be explained by a few uncorrelated vectors for easier understanding of the trends in the dataset and subsequently building stronger predictive models. Therefore, chemometric analysis usually in the classic form of principal component analysis (PCA) and the partial least squares (PLS) regression is essential to process the multivariate NIR data.

PCA remains the primary statistical procedure to reduce the complexity and to redefine the multidimensional data by using a set of orthogonal vectors called principal components (PCs). The data points are then projected onto a new coordinate system with PCs axes in order to explain the largest possible variance within the data and to classify the observations (Jolliffe and Cadima, 2016). The first principal component (PC_1) is a vector that passes through the long axis of the data

cloud corresponding to the maximum variance within the data in its direction. The second principal component (PC_2) is then created perpendicular to the first one in the direction of the next highest variance with intersection at the centroid of the mean-centered data. Each successive PC explains the remaining portion of the variability in their respective orthogonal direction to the other PCs.

In pharmaceutical applications, usually a high portion of the variations in the NIR spectra can be expressed using only a few PCs. PCA models with higher number of PCs are considered as overfit models which may not necessarily equate to higher predicting qualities. Such complex calibration/training models usually fail when they are validated using independent datasets, even though they may have high regression coefficient (R^2) and a small root mean square error of cross–validation (RMSE*cv*) (Reich, 2005).

2.4.4.2.1. PLS and OPLS regression methods

PLS regression is a well-known, well-described and widely used multivariate data analysis method that accounts for multicollinearity (highly correlated variables) and missing values in the variable/predictor matrix X for making reliable regression coefficients (Homayoun et al., 2011). PLS as a mathematical model starts with the assumption that *there is* a meaningful interrelationship between the two matrices of X and Y and then tries to find the best possible tactic to link the two matrices so it can finally be able to predict the outcome Y from X (Erikson et al., 2013). As opposed to PCA which only explains the variations within the X matrix, PLS explains the systematic variations in the X matrix that are related to the variations in the Y matrix (Sadeghi-Bazargani et al., 2011).

Trygg and Wold (2002) introduced orthogonal projections to latent structures (OPLS) as a modification to PLS. The OPLS method can further maximize the explained covariance between X and Y matrices by excluding the orthogonal or systematic variations in X that was not linearly correlated to Y and explaining such variations separately. The portion of the variables in the X matrix that contribute directly towards predicting the Y is modeled independently and a new vector 'R^2x (predictive)' is introduced instead of the PC_1 in the PLS method. Thus, OPLS offers an advantage over the more traditional PLS method by reducing the model complexity, excluding non-correlated variation in the X matrix and more importantly improving the interpretation of the data. OPLS also adjusts the projection of the observations in the score plot of the PLS with enhanced separation between different classes so that partitioning of the observations would be more consistent with the chemical assumption behind the experimental design of experiments (DOE). In NIR spectroscopic analysis using a single column Y matrix, the OPLS method 'rotates' all the relevant predictive information into only the first axis (R^2x (predictive)) on the score plot so that the systemic separation between the

observations would align properly with the linear increase of the API dose in one direction.

However, in the single Y scenario, which is usually the case for spectroscopic data, both PLS and OPLS are absolutely identical and there is no distinction between the predictive abilities of such techniques.

3. Aims of the study

This thesis was focused on two main topics. The first objective was to study the manufacturing of uniform and accurately tailored doses of oral dosage forms using inkjet printing technologies for precision medicine. The second and main objective was the investigation of various analytical techniques in quality control of the printed formulations.

In addition, the molecular-level interactions between the drug and the excipients, the solid-state properties of the drugs in the formulations and the degradation tendency of the drugs under different storing conditions were studied. Complementary techniques were also applied to various extents for each project to further study the effect of printing on the substrates and the mechanical and disintegration properties of the produced orodispersible formulations.

The specific objectives in more detail were to:

- Gain a deeper and more insightful understanding of the physicochemical properties and interactions of different drug substances in the various ink solutions when printed on different carrier substrates.

- Develop and study the quality of ion-selective electrodes (ISEs) using the potentiometric analysis for the study of drug release from different polymeric films and cellulose-based porous substrates.

- Study the integrated use of inkjet and flexographic printing technologies to produce accurately dosed medicine with control over the drug release profiles by polymeric coating of already inkjet printed formulations.

- Investigate the feasibility of hyperspectral NIR imaging together with chemometrics to build quantitative predictive models as well as qualitative concentration maps to allow digital and visual assessment of both the API amount and the uniformity of its distribution on inkjet printed systems.

- Study the use of a handheld colorimetric device for indirect measurement of the API dose in printed orodispersible delivery systems for pediatrics.

- Investigate the application of a compact handheld NIR probe for prediction of the drug dose on different edible substrates with the potential to be installed in-line in a continuous manufacturing scenario.

4. Materials and methods

4.1. Materials

4.1.1. Active pharmaceutical ingredients

Propranolol hydrochloride (Sigma, St. Louis, MO, USA and Fagron, Copenhagen, Denmark) (I, II, IV), lidocaine hydrochloride monohydrate (Sigma, St. Louis, MO, USA) (I), riboflavin sodium phosphate (RSP, riboflavin 5´-monophosphate sodium salt, Ph. Eur., Fluka Analytical, Sigma–Aldrich, France) (II), anhydrous theophylline 200 M (Orion Pharma, Espoo, Finland) (III), levothyroxine sodium salt pentahydrate (≥98%, Sigma–Aldrich Co., Italy) (V) and prednisolone (≥99%, Sigma–Aldrich Co., China) (V) were all used as the model APIs **(Figure 4)**.

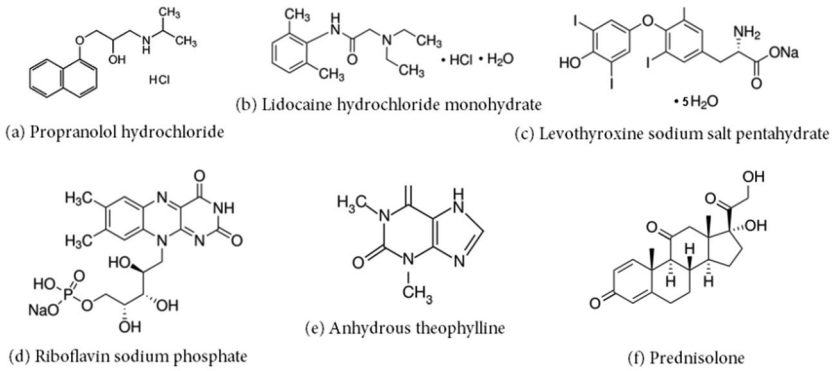

Figure 4. *Chemical structures of the APIs.*

4.1.2. Excipients

Ethylcellulose (EC, Sigma, St. Louis, MO, USA; ethoxy content, 48–49.5%; viscosity, 45 cP) (I-II) A), hydroxypropyl cellulose (HPC, Shin-Etsu, Japan (I, V) and Klucel® EXF, Ashland, Wilmington, DE, USA (IV)), hydroxypropyl methylcellulose (HPMC, Pharmacoat® 606, Shin–Etsu, Wiesbaden, Germany) (V), propylene glycol (PG, ≥99.5%, Sigma–Aldrich, Germany) (II, V), glycerol (≥99.5%, J.T. Baker, Deventer, Holland) (II, IV, V), saccharin sodium salt hydrate (≥98%, Sigma–Aldrich Inc., USA) (IV) and edible ink (V) which was consisted of water, glycerol (E422), brilliant black (E151), sunset yellow (E110), tartrazine (E102), ponceau 4R (E124), azorubine (E122), brilliant blue FCF (E133), propylene glycol (E1520) and citric acid (E330) (Deco Enterprises Ltd, London, UK) were used as model excipients. Potassium dihydrogen phosphate and hydrochloric acid (≥37%, Sigma–Aldrich Inc. (St. Louis, MO, USA) (I, IV) were used for the preparation of assay and dissolution media. Ethanol (≥96.1%, Etax A, Altia OYj, Finland) and double-distilled water (Milli-Q) (I-IV) were used as solvents throughout this entire study.

4.1.3. Commercially available substrates

Uncoated filter paper (138 g/m^2, Whatman International Ltd, Maidstone, England) (I), alkyl ketene dimer-sized uncoated woodfree paper (A), triple-coated inkjet paper (B) and double-coated sheet fed offset paper (C) (Sappi Fine Paper Europe, Brussels, Belgium) (II), uncoated copying paper (Optitext, 80 g/m^2, Stora Enso Oyj Fine Paper, Oulu, Finland) (III), edible icing sheet (EIS, Sutton Valence, Kent, UK (IV) and Culpitt Ltd, Ashington, UK (V)) and edible rice paper (ERP, N.J. Products Ltd, Birstall, UK) (IV) were used as commercially available porous carrier substrates.

4.1.4. Electrodes membrane

Polyvinyl chloride (PVC), 2-nitrophenyl octyl ether (NPOE), potassium tetrakis(4-chlorophenyl) borate (KTpClPB) and tetrahydrofuran (THF) were all Selectophore reagents from (Fluka, Hauppauge, NY, USA) (I) which were used for preparation of ISE membrane cocktail along with carbon cloth (Kynol® activated carbon fabric ACC-5092-20, Kynol Europa GmbH, Hamburg, Germany) (I).

4.2. Methods

4.2.1. Preparation of polymeric substrates by solvent casting

In addition to the commercially available substrates, 2 types of blank polymer substrates were prepared manually by solvent casting using a film applicator multicator 411 with 220 mm gap width and wet coating thickness of 500 µm (Erichsen, Hemer, Germany). In paper (IV), a film containing HPC:ethanol (15:85 w/w%) was applied on top of the edible rice paper (ERP) to create a modified carrier substrate and in paper (V), a polymer film containing HPC:HPMC:glycerol:ethanol (7.5:7.5:5:80 w/w%) was prepared on top of an impermeable transparency film (Dataline™, Transparency film, code 57170, EU) which only served as liner and later was detached from the polymer film during analysis (V). The created substrates were dried in ambient conditions (20 ± 5% relative humidity (RH) and 24 ± 1 °C) for 24–48 h before printing.

4.2.2. Preparation of formulations (I–V)

4.2.2.1. Drug-polymer solvent casting (I)

Nine drug-polymer solutions with different compositions containing 2 APIs and 2 polymers of various weight ratios were prepared. All the solutions were subsequently drop-casted by a pipette into a Teflon mold (Ø 20 mm) to create 9 different thin-film formulations and three of these solutions were drop-casted by the pipette onto the surface of the uncoated porous cellulose-based substrates (Ø 28 mm) to create 3 additional formulations for paper (I) (n = 3) **(Figure 5)**. In order to accomplish this, the mixed powder of the drug and polymers were first dissolved in ethanol with the ratio of 1 g in 5ml of the solvent at 60 °C in an ultrasound bath for 15 min. 1 ml of

each drug-polymer solution was then used for the making of each film on the Teflon mold and 0.5 ml of this solution was deposited on the porous cellulose substrates. The created formulations were left to dry in a desiccator containing silica gel at room temperature for 24 h before starting the dissolution measurement.

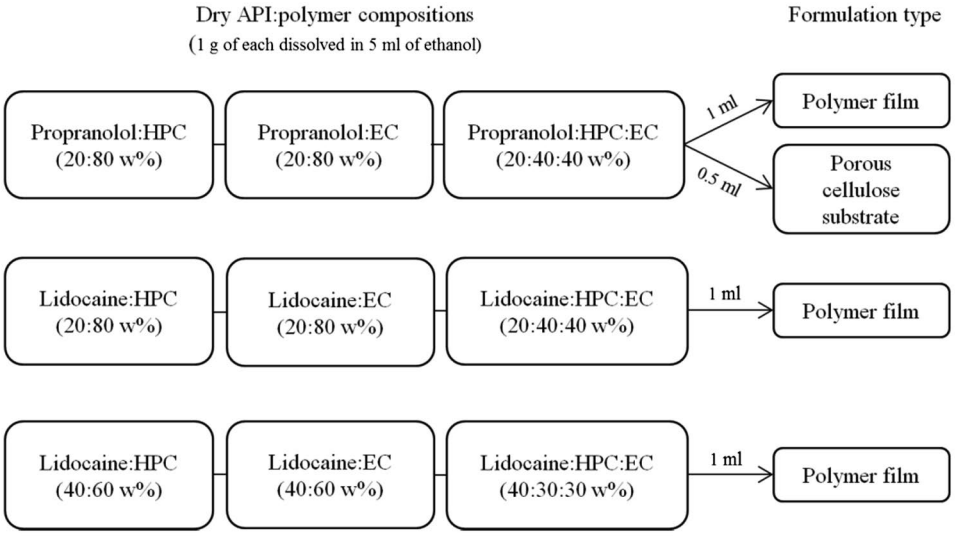

Figure 5. *Different manually designed formulations for paper (I).*

4.2.2.2. Dimatix and flexographic inkjet printing (II)

A Dimatix DMP-2800 inkjet printer (Fujifilm Dimatix Inc., Santa Clara, California) with a MEMS-based cartridge-styled printhead which had 16 nozzles linearly spaced at 254 µm to produce a typical drop size of 10 pl was used to inkjet print formulations containing propranolol hydrochloride and riboflavin sodium phosphate for paper (II). The ink solutions were 50 mg/ml propranolol powder in PG:water mixture (30:70, vol%) and 31.5 mg/ml of riboflavin powder in glycerol:ethanol:water (10:10:80, vol%). The ink solutions were filtered into each ink cartridge with a volume of 1.5 ml at 30 ˚C using 0.45 µm and 0.2 µm polypropylene membrane filters (Whatman™, GE Healthcare, Piscataway, NJ, USA). Printing was performed on squared areas of 1 cm^2 (n = 10-20) on the substrates using a single nozzle (Ø 20 µm) with drop spacing of 10 µm and firing voltages of 30 V and 35 V for propranolol and riboflavin, respectively. According to the Dimatix software the total number of 1,002,001 drops with a drop volume of 10 pl were deposited onto a 1 cm^2 area of each substrate which was theoretically corresponding to approximately 10.02 µl/cm^2. The theoretical printed drug amount was calculated to be 0.501 mg for propranolol and 0.316 mg for riboflavin formulations.

A laboratory scale printability tester (IGT Global Standard Tester 2, IGT Testing system, The Netherlands) was used for contact flexographic printing of a polymer coating ink consisting of EC:ethanol (5:95 w%) on top of the already Dimatix

printed formulations for paper (II) **(Figure 6)**. The coating polymer was applied locally to a small area of the anilox roll with a cell angle of 45˚, a cell volume of 20 ml/m^2 and a line count of 40 l/cm. The rotating anilox roll was in contact (P = 100 N) with the plate roll with a selected relief pattern on its surface as the printing template. The plate roll was also in contact (P = 50 N) with the impression roll with the earlier Dimatix printed substrates attached to its surface. During printing the anilox roll rotated at the printing speed of 0.5 m/s in order to distribute the ink evenly on its surface while the excess coating ink was removed by the doctor blade. Through one spin of the rotating system, the polymer ink was transferred from the anilox roll onto the relief pattern of the printing plate and subsequently was coated as one layer on the substrate. The formulations were coated on both sides with 5 and 30 layers of EC solution to study the effect of the polymer coating on the drug release. All the printings procedures were carried out in ambient conditions (45 ± 5% relative humidity (RH) and 21 ± 2 ˚C).

Figure 6. *The flexographic printing unit.*

4.2.2.3. Thermal and piezoelectric inkjet printing (III–V)

Concentrated API containing ink solutions were used to fill empty black cartridges of commercially available desktop thermal inkjet printers and the refillable container of the piezoelectric inkjet printer. A solution of 20 mg/ml of anhydrous theophylline in glycerol:water:ethanol (10:45:45 vol%) was replaced in the cartridge of a Pixma MP495 (Canon Inc., Japan) (III). A solution of 50 mg/ml propranolol hydrochloride ink solution in a mixture of water:glycerol (90:10 vol%) was transferred in the cartridge of a Pixma iP7250 (Canon Inc., Japan) (IV). Solutions of 40 mg/ml prednisolone and 20 mg/ml levothyroxine sodium in DMSO:ethanol:PG (45:45:10 vol %) were used as separate inks on a PixDro LP 50 piezoelectric inkjet printer (Roth & Rau, Eindhoven, Netherlands) (V). Glycerol and PG were added to the ink solutions as moisturizing agents, viscosity modifiers and to prevent the nozzles from blocking. All the ink solutions were filtered with 0.2 mm polypropylene membrane

filters (What-manTM, GE Healthcare, Piscataway, NJ, USA) before printing. In order to achieve escalating dose systems, multiple superimposed layers (1-32) were printed with thermal inkjet printers (III-IV) while different print resolutions (from 500 × 500 dpi to 1000 × 1000 dpi) were used to obtain the escalating drug doses when using the piezoelectric inkjet printer (V).

The printing parameters on thermal inkjet printers were set to normal print quality and resolution. The printing parameters for the piezoelectric inkjet printer were set as follows: a Spectra® SL–128 AA printhead with 128 nozzles (Ø 50 µm) and spacing of 508 µm; the ink pressure and the jetting voltage were set at −18.30 mbar and 85 V, respectively; the time to reach the fixed voltage was set at 3 µs, the time period of applied voltage on the piezoelectric element was between 17–18 µs and the time for the voltage drop was set between 3–4 µs.

The drug delivery systems were printed on squared areas of 1 cm^2, 2 cm^2 and 4 cm^2 on different substrates according to the templates that were digitally designed in Microsoft Power Point 2010 (Microsoft Inc.).

4.2.3. Texture analysis and disintegration time of substrates (IV–V)

Tensile strength (N/mm^2), puncture resistance (kPa), distance at burst (mm) and elongation percentage of the substrates were measured before and after printing by a TA.XT plus texture analyzer (Stable Micro Systems Ltd., Surrey, UK). For tensile strength measurement, a self–tightening roller grips probe was attached to both ends of the substrates and the maximum force (N) at the point of break was divided by the cross–sectional area (mm^2) of each substrate to calculate the tensile strength. For puncture resistance measurements, a spherical stainless steel probe P/5 (Ø 5 mm) was attached to the load cell and was lowered to puncture the substrate that was held in place by a set of clamping rings (Ø 1 cm). The resistance (kPa) of the substrates against the perpendicular penetration of the probe on the circular area as well as the distance of penetration (mm) at which the first fracture (puncture) appeared on the surface of the substrates were reported. The speed of the moving tensile and the puncture probe were set to 1 mm/sec. (n=10).

The system for the disintegration test included a sample holder unit clamped on the top corner of the substrate with the area size of 2 cm^2. Preis et al. (2014) suggested that a force of 0.03 N could approximate the minimal force applied by human tongue when licking on a probe. Therefore, different weights of 1, 3 and 5 g were attached to the bottom corner of the substrate to simulate the exerting force of the tongue. The substrate was then gently introduced into a phosphate buffer medium (pH 6.0) as the starting point for the disintegration test. The time period for the bottom half of the substrates to break apart after entering the buffer medium was recorded and reported as the disintegration time (n=10). The temperature of the buffer medium was maintained at 37 ± 0.5 °C, while the relative humidity (RH)

during the experiments was recorded to be 45 ± 5 % for paper (IV), while these conditions were 23 ± 1 °C and below 15 % RH for paper (V).

4.2.4. UV spectroscopy for content and dissolution analysis (I–V)

The making of the calibration plots, the drug content measurements and the dissolution analyses of the formulation units were performed using four different UV-Vis spectroscopic devices throughout this thesis. Each solution was incubated for at least 2 h in a buffer solution medium (pH 1.2 and 6; T = 20 ± 5 ˚C for assay and 37 ˚C for dissolution). The incubated solutions were filtered with 0.2 μm polypropylene membrane filters before the measurements in a transparent cuvette with a path length of 1 cm. The maximum absorbance values of each drug were recorded at a specific wavelength known as the wavelength of maximum absorbance.

A PerkinElmer UV-Vis spectrophotometer (Lambda 25, USA) was used for measurements of lidocaine hydrochloride (λ = 263 nm), propranolol hydrochloride (λ = 289 nm) and riboflavin sodium phosphate (λ = 267 nm) samples (I and II); a Cary 50 UV–vis spectrophotometer (Varian Medical Systems, Inc. Palo Alto, California, USA) for theophylline anhydrous (λ = 213 nm) (III); a Ultrospec 2100 pro spectrophotometer (Biochrom Ltd, Cambridge, England) for propranolol hydrochloride (λ = 289 nm) (IV) and a NanoDrop 2000c UV–Vis Spectrophotometer (Thermo Scientific™, MA, USA) was used for prednisolone (λ = 248 nm) measurements (V).

4.2.5. HPLC Content analysis (V)

The calibration plot and the levothyroxine sodium (λ = 225 nm) content of the formulations were measured using a Merck HITACHI LaChrom series HPLC (Tokyo, Japan) consisting of a quaternary pump, an automatic injector, a variable wavelength detector and a column oven. Data were collected using Merck HITACHI D–7000 HPLC system manager and Chromatography Data Station software. The separation of the drug-excipient mixture was achieved using a Phenomenex C18 column (Gemini–NX, 100 x 4.6 mm, 3μm) fitted with a Phenomenex guard column (C18 4 X 2.0 mm). The mobile phase was consisting of A: 0.01M Phosphate buffer (pH 3.0) and B: Methanol (100%) with a flow rate of 1.0 ml/min. The chromatographic gradient was consisting of solvent 45–20% A in the first 7 min, at 20% A from 7 to 12 min, 20–45% A from 12 to 16 min and at 45% A until 20 min (Collier et al., 2010). The column temperature was fixed at 30 °C. The injection volume was 50 μl. A solution of water:methanol (95:5 vol%) was used as the assay medium. Samples were filtered with 0.2 μm polypropylene membrane filters.

4.2.6. ISEs and the potentiometric measurements (I)

For paper (I), the potentiometric measurements were carried out with an EMF 16 Interface potentiometric device (Lawson labs, Inc., Phoenixville Pike, USA) in a 100

ml buffer solution (pH 1.2) as the dissolution medium while stirring at 300 rpm with an IKA® RCT hotplate magnetic stirrer (Staufen im Breisgau, Germany) at 37 ˚C.
The reference electrode was a conventional single junction electrode (Metrohm, Switzerland) consisted of an Ag/AgCl wire in an enclosed solution of 3 M KCl. The small-scale solid-contact ISEs were manually designed by the author and were used as working electrodes. The outer body of the electrodes was made of hollow PVC cylinders. Carbon cloth (Kynol® activated carbon fabric ACC-5092-20, Kynol Europa GmbH, Hamburg, Germany) was used as the ion-to-electron transducer material inside the hollow cavity of the cylindrical electrode bodies **(Figure 7)**. The carbon cloth was connected to the potentiometric device at one end and the solid electrode membrane at the other end which is usually immersed in the conditioning/measuring solutions. The electrode membrane cocktail (450 µl) was consisting of PVC:NPOE:KTpClPB (33:66:1 w%) that were dissolved in THF as the solvent with the ratio of 1:5 w%. Portions of 100 µl membrane cocktail were drop-casted directly on one end of the electrodes in time intervals of 30 min for practical reasons. The membranes were air dried at room temperature for 2 days. Three parallel ISEs were prepared **(Figure 8)** and each were conditioned for 3 weeks prior to measurements in separate diluted HCl solutions (pH 2) containing propranolol hydrochloride (0.295 mg/ml) and lidocaine hydrochloride (0.267 mg/ml).

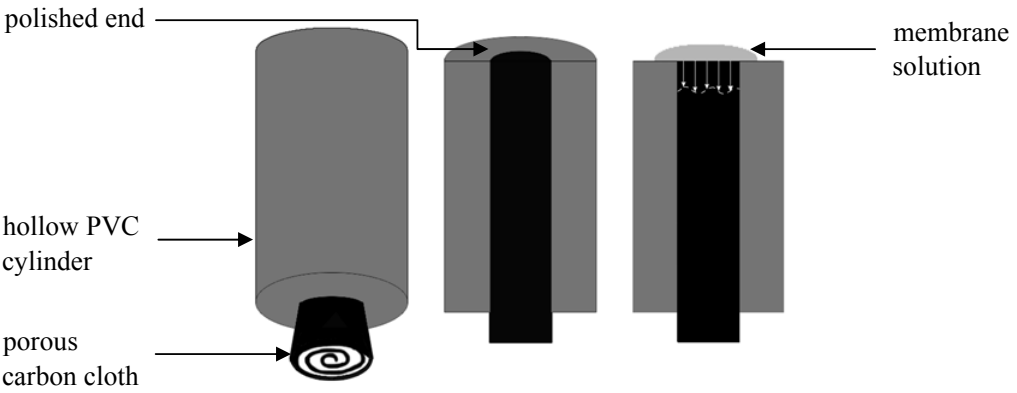

Figure 7. *The schematic of the ISEs. Left: hollow PVC cylinder with carbon cloth inserted inside; middle: top view with the polished end and right: the membrane cocktail deposited onto the polished end and diffusing into the carbon cloth.*

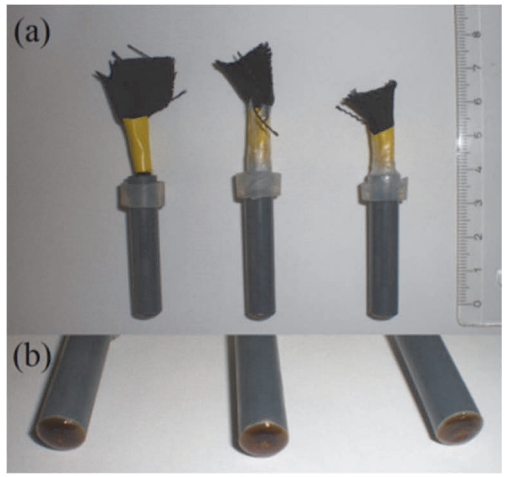

Figure 8. *(a) The manufactured ISEs and (b) the view of the solid-contact membrane at the tip of the electrodes.*

4.2.7. Hyperscpectral NIR imaging (III)

For paper (III), a push-broom SisuCHEMA hyperspectral imaging instrument (SPECIM, Spectral Imaging Ltd. Oulu, Finland) equipped with a SPECIM mercury cadmium tellurium (MCT) based spectral camera for optimal sensitivity and signal-to-noise ratio was used to collect the NIR image of the entire escalating system of printed theophylline anhydrous formulations **(Figure 9)**. The obtained image quality was 256 × 320 pixels with 0.3125 mm spatial resolution per pixel for a sample with 100 mm width. The spectral range of 942–2542 nm with steps of 6.25 nm including 256 individual spectral bands was collected for each pixel resulting in 81920 separate spectra for the image in less than 7 seconds.

Figure 9. *SisuCHEMA hyperspectral imaging device (SPECIM, Oulu, Finland).*

4.2.7.1. Hyperspectral data cube pre-treatment and PLS regression model

All the data acquisition, pre-processing and multivariate analysis were performed using the Evince Image software (UmBio Umeå, Sweden). The collected spectral range was reduced to 1000–2500 nm to mask the anomalies, artifacts and the noise that were extremely deviating from the main data cloud on t_1/u_1 score plot. The reflectance hypercube data was mean centered and treated with standard normal variate (SNV) scatter correction prior to multivariate analysis. PCA was used to classify the collected observations on the pixel level into color coded images in order to visualize the interrelationships within the data. A PLS calibration model was then created based on 4 of the separate printed unit areas for prediction of the API content. Each printed unit on PCA contour 2D plot was then correlated to their equivalent API content that was measured earlier by the UV spectroscopic technique. The software allows the user to select an area down to pixel levels to predict the corresponding drug amount in that specific location.

4.2.8. Colorimetry measurements (IV)

For paper (IV), a CLM-194 handheld digital tristimulus colorimeter (EOPTIS, Trento, Italy) **(Figure 10)** was used with an integrated LED illuminator and the measurement area of 10 mm in diameter. The CLM-194 Interface software associates each color to a single parameter known as 'color difference (ΔE*ab)' in the three dimensional CIELAB color space. Color difference values are in fact the 3D Euclidean distance between the 3 numerical values of L*, a* and b* recorded from each of the printed units and the same numerical values measured from a reference color of only one printed layer. The circumferential geometry (45° C:0°) was selected according to ASTM E 1164 standard to exclude the undesired specular component (gloss). CIE standard illuminant D65 and CIE 1931 2° standard colorimetric observer were selected for illuminant-observer pair selection. The samples were studied on reflective mode for all the measurements under the same condition (n = 3). The graphical color distribution maps of the printed formulation were presented in CIELAB color space for the three different substrates. Moreover, the validation plots of ΔE*ab values vs. number of printed layers were reported.

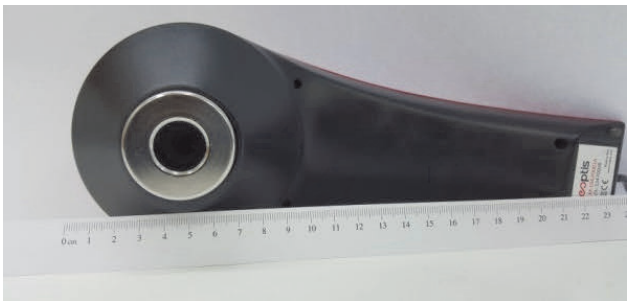

Figure 10. *The CLM-194 handheld colorimeter (EOPTIS, Trento, Italy).*

4.2.9. NIR data collection (V)

For paper (V), a compact handheld high–performance NIR spectral device N2.0 (Spectral Engines Oy, Helsinki, Finland) **(Figure 11)** with single element extended indium gallium arsenide (InGaAs) detector was used to collect the NIR absorbance spectra in the range of 1550–1950 nm with 5 nm steps. The NIR illumination source was made of two tungsten vacuum lamps which were set to 50% of the lamps voltage during the measurements. The reflected NIR light was collected through the detection aperture (Ø 1 mm) in the center at 2 mm above the surface. One spectrum was collected from a random spot on the surface of each parallel printed unit containing prednisolone or levothyroxine sodium.

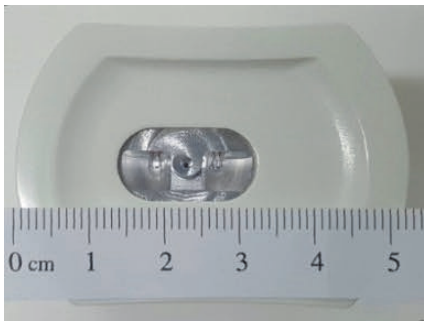

Figure 11. *The handheld NIR probe (Spectral Engines Oy, Helsinki, Finland).*

4.2.9.1. NIR data treatment and modeling

The obtained NIR spectra was imported to SIMCA® 14.1 software (MKS Umetrics, Umea, Sweden) for systematic data treatment to standardize the modelling method. The spectra were mean centered without scaling and a Savitzky–Golay (SG) smoothing technique was applied to the data prior to analysis using a 15-points window width and a quadratic polynomial approach. Having considered all the combinations of all available scatter correction and derivative techniques in the software, a SG approach with the 3rd derivative using 15 points and 2nd order polynomial smoothing function was selected for the models. Principal component analysis (PCA) and orthogonal projections to latent structures (OPLS) were executed on datasets to classify the observations and to build predictive models based on the filtered and numerical differentiated data. For authentic validation, each dataset was partitioned into a training set and a validation set to evaluate the predictive ability of each model. The goodness of prediction (Q^2), the goodness of fit (R^2), the predictive portion of the variables R^2X (predictive), the cumulative sum of explained variables (R^2X (cum)), the number of principal components that best described each model as well as RMSE*cv* values were reported. Subsequently plots of raw and differentiated spectra, scatter score plots and plots of observed vs. predictions were presented for each model.

4.2.10. SEM and EDX analysis (IV, V)

A SEM (LEO Gemini 1530, Oberkochen, Germany) equipped with a thermo scientific ultra-dry silicon drift detector was used to study the surface morphology of the blank and the printed substrate for paper (IV) and paper (V). All samples were coated with carbon by using a vacuum evaporator prior to scanning. SEM images were obtained at an accelerated voltage of 8 kV with 100× and 2500× magnifications. The images were taken using the secondary electron detector while the pressure was kept constant at 2×10^{-5} mbar during scanning.

Energy-dispersive X-ray analysis (EDX) was performed in extension to SEM by using an energy-dispersive spectrometer (Thermo Scientific, Madison, Wisconsin, USA) in order to identify the elemental composition of various regions on the surface of the printed units for paper (V). The EDX analysis was carried out with magnifications of 500× and 1000×, image resolution of 1024 × 768 and image pixel size of 0.12–0.24 mm at an accelerated voltage of 15 kV.

4.2.11. Scanning white light interferometry (SWLI) (II, IV)

A custom-made SWLI instrument with a NIKON reflective microscope frame (6.3× magnification) equipped with a 10x MIRAU interferometry objective (NIKON IC Epi Plan DI, Japan), a 100 µm piezoelectric z-scanner (Physik Instrumente P-721 PIFOC®, Karlsruhe, Germany), a high-resolution CCD camera (Hamamatsu Orka Flash 2.8 CMOS, Hamamatsu City, Japan), a standard halogen lamp as the white light source and two motorized translation stages (STANDA 8MTF-102LS05, Vilnius, Lithuania) was used to study the surface topography of the printed formulations for paper (II) and (IV). The scanning and the data collection were achieved with a C++ based software built in-house. The 3D-image construction and the 3D-data analysis were performed using the commercial MountainsMap® Imaging Topography 7.2-software (Digital Surf, Avencon, France). The surface roughness (Sq) values were calculated according to ISO 25178 standard (n = 3).

4.2.12. ATR–IR (IV, V)

An attenuated total reflectance infrared (ATR–IR) Spectrum Two spectroscopic instrument (PerkinElmer, UK) with a single reflection artificial diamond ATR crystal was used to collect the infrared spectra of the raw substrate, the printed formulations and the API containing inks in the region of 450–4000 cm^{-1} to study the solid-state of the drug after printing and the stability of the ink during a 24 h period for paper (IV) and (V). A force gauge of 75–80 N was applied to the films during the analysis. The baseline was corrected for all the spectra. All the ATR-IR spectra were obtained with a 4 cm^{-1} resolution.

4.2.13. DSC measurements (IV, V)

A differential scanning calorimetric (DSC) instrument (Q2000, TA Instruments Inc., USA) was used to study the solid-state properties of the drug and its possible recrystallization in the formulations after the storage time. Pure drug powder and printed samples of 1.5–6.4 mg were subjected to a heat ramp of 10 ˚C/min from 40 ˚C to 200 ˚C in Tzero aluminum pans and lids with a flow of 50 ml/min nitrogen gas in the furnace chamber.

5. Results and discussion

5.1. General remarks

This research shows the clear advantages of various inkjet printing technologies to manufacture precise and uniform doses of drugs on ODFs for precision medicine. Additional polymeric coatings were applied to the printed formulations using either a coating knife or by flexographic printing to investigate the effect of coating on the drug release profiles as well as for higher palatability purposes. Furthermore, surface morphology, surface roughness, mechanical properties, disintegration behavior, solid-state properties and stability of the printed formulations were examined to various extents in each project.

The present thesis applied the latest analytical advancements in the field to investigate the possibilities of their application as fast, low-cost and reliable alternatives to the conventional methods of quality control that are currently available for the new printed formulations. The robust SC-ISEs were used as an inexpensive and powerful alternative to UV spectroscopic methods for drug release studies of the solvent-casted formulations. The hyperspectral NIR imaging technique provided an easy-to-interpret visual quality control approach to simultaneously predict the content and the spatial distribution of the API in the printed formulations. A colorimetric instrument was used to estimate the API content of the escalating dose systems on different edible substrates that were produced by thermal inkjet printing. Finally, a handheld NIR spectrometer was used along with multivariate data analysis techniques to predict the amount of two poorly soluble APIs on different edible substrates.

5.2. Visual characterization of the printed dosage forms

It is highly important for the reader to visualize the shape and the morphology of the printed dosage forms for better understanding of the discussions regarding such formulations. The formulations were printed on several edible and inedible substrates/carriers in the shape of squares of different area sizes (1, 2 or 4 cm^2) for different projects. The dose tuning was achieved either by printing multiple layers or by variation in the print resolution in terms of drops per inches (dpi). **Figure 12** shows an example of a digital camera image of one set of printed formulations that was prepared by piezoelectric printing for paper (V) to demonstrate the physical appearance of a typical printed system. The red coloring agent was added to the ink solely for the visualization purpose.

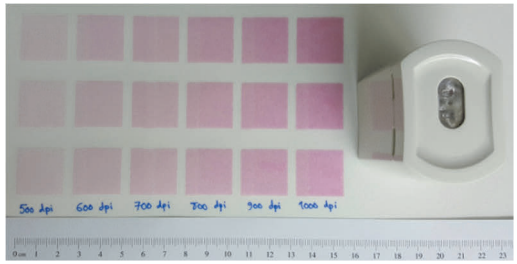

Figure 12. *A typical set of printed formulations on edible icing sheet substrate and the NIR probe.*

The surface morphology of the blank and printed substrates was visualized on 4 substrates by scanning electron microscopy (SEM) for paper IV and V (**Figure 13)**.

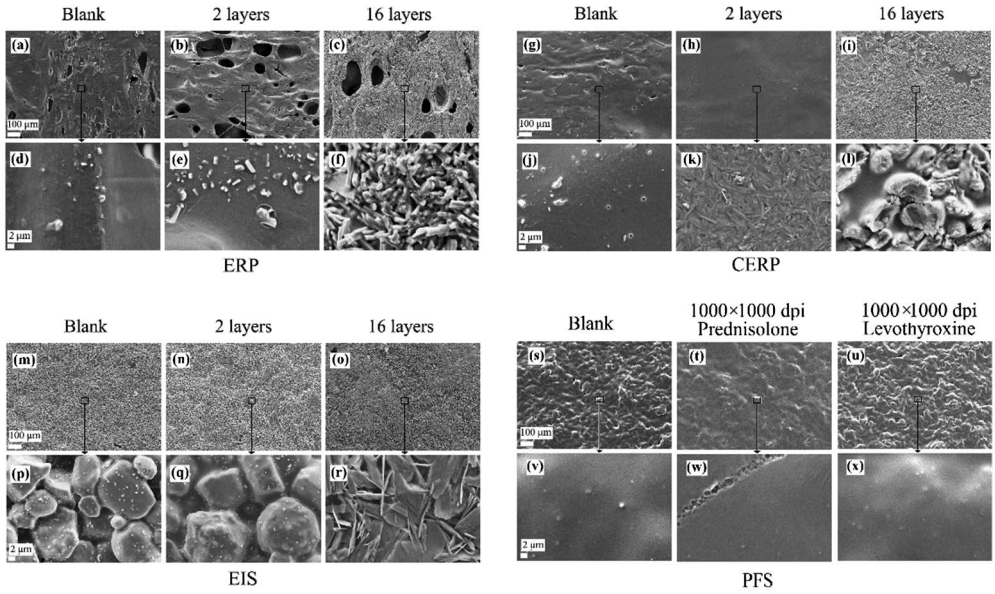

Figure 13. *Scanning electron microscopy images of various printed formulations with magnifications of 100× (100 mm scale bar) and 2500× (2 mm scale bar).*

The porous structure and the cavities of variable sizes were detected for the edible rice paper (ERP) that contained potato starch and vegetable oil **(Figure 13(a) and (d))**. The structure of this substrate became even more fractured as the number of printing layers increased and the ink started to interact with the starch matrix to form a coarse surface in case of the highest printed layer **(Figure 13(b) and (c))**. The smooth surface of the coated edible rice substrate (CERP) **(Figure 13(g))** was transformed to a more uneven surface after 2 layers of printing **(Figure 13(h) and (k))** and as printing layers increased to 16 layers **(Figure 13(i) and (l))** the HPC coating layer fragmented and formed irregular aggregates. The glucose particles on

the surface of the blank edible icing sheet (EIS) **(Figure 13(m) and (p))** were observed. The white spots on the glucose particles were of titanium origin which was a constituent of this substrate. The particles were covered by a thin layer of ink after 2 printing layers **(Figure 13(n) and (q))** and as printing continued, the sugar components were recrystallized to rod-like crystals **(Figure 13(o) and (r))**. Printing on the polymer film substrate (PFS) **(Figure 13(s) – (x))** did not appear to make any noticeable changes on the smooth surface of this substrate.

The complimentary EDX analysis was conducted on randomly selected areas on the surface of each sample in order to detect chlorine element distribution as an indication for presence of propranolol hydrochloride in the printed units. As expected, higher amounts of chlorine were consistently detected on areas with higher doses with a standard deviation lower than 1.4 w% which was yet another confirmation of the uniformity of the printing job (results in publication IV).

5.3 Content uniformity of inkjet printed formulations (II–V)

The drug deposited amounts on different substrates as the result of inkjet printing techniques were measured by UV spectroscopic (II–V) and HPLC (V) techniques.

The results for paper (II) showed that the average amount of propranolol deposited by the Dimatix piezoelectric inkjet printer on a 1cm^2 area was 0.503 ± 0.003 mg, which was in close alignment with the expected theoretical value of 0.501 mg. Also, the amount of riboflavin in a printed square was found to be 0.340 ± 0.002 mg, which was slightly higher than the estimated theoretical value of 0.315 mg. The higher deposition of riboflavin ink was attributed to its 50% lower viscosity compared to propranolol ink, since the surface tension values of both inks were nearly identical.

For paper (III), anhydrous theophylline was printed using a thermal inkjet printer on 1 cm^2 areas of an uncoated copying paper in an escalating system of 1–32 printing layers. The results showed that the average drug amount of 7.53 ± 0.37 μg was achieved for each printed layer. Additionally, an accurate escalating dose window of 7.44–246.83 μg was tailored in which the drug dose was directly proportional to the number of printed layers with excellent fit accuracy of R^2 = 0.9998 **(Figure 14 (a))**.

For paper (IV), propranolol hydrochloride was printed with a thermal inkjet printer on 3 different edible substrates and on 3 different area sizes of 1, 2 and 4 cm^2 on each substrate in escalating systems of 2–16 printing layers. The results showed that the average drug amount of 49.78 ± 0.01 μg per layer per 1 cm^2 area was achieved. The dose in all the printed units was directly proportional to the number of printed layers and the printed area with the fit accuracy in the range of R^2 = 0.993–0.999 **(Figure 14 (b))**.

For paper (V), prednisolone and levothyroxine sodium pentahydrate were printed on 2 different edible substrates in an escalating manner that was based on an

escalating print resolutions system (500 × 500 to 1000 × 1000 dpi) by the piezoelectric inkjet printer. The amount of drug load on substrates was once again in good agreement ($R^2 \geq 0.997$) with the increase in the print resolution **(Figure 14 (c))**.

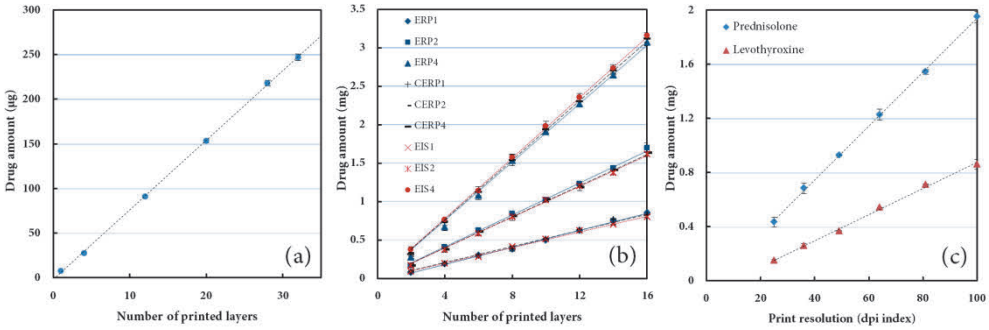

Figure 14. *The dose flexibility of the printed formulations. (a) Theophylline (III); (b) propranolol (IV) and (c) prednisolone and levothyroxine (V).*

In summary, thermal and piezoelectric inkjet printing techniques were able to accurately deposit different drugs on various substrates in µg range. The deposited drug amount depends on the concentration of the drug in the ink solution, the size of the printed area and the viscosity and the surface tension of the ink as well as the printing parameters. The extremely high accuracy ($R^2 = 0.9998$) of the drug amount with respect to the number of printed layers on uncoated copying paper (III) was related to the enhanced printing qualities of such substrate which could greatly absorb and retain the drug in ink solution. The usual 'smearing effect' of the printed ink when using a contact thermal inkjet printer with mechanical handling of the feed paper, was not observed for this substrate because of its excellent qualities and specific design for printing. Moreover, the non-contact piezoelectric inkjet printing (V) technique resulted in a very accurate and uniform deposition of prednisolone with respect to the print resolution ($R^2 = 0.9994$).

5.4 Dissolution studies (I, II)

For paper (I), the dissolution profiles of 2 APIs, propranolol hydrochloride and lidocaine hydrochloride, from different drug-polymer systems were measured by the potentiometric method to study the effect of composition and the type of formulation in the drug release behavior. Two different polymers, EC and HPC, with a substantial difference in aqueous solubility were used with different mass ratios of (1:0, 1:1 and 0:1) to produce two types of delivery systems including polymer films and porous substrates. The dissolution profiles of the formulations showed major differences in drug release kinetics according to the composition and the type of the formulations **(Figure 15)**.

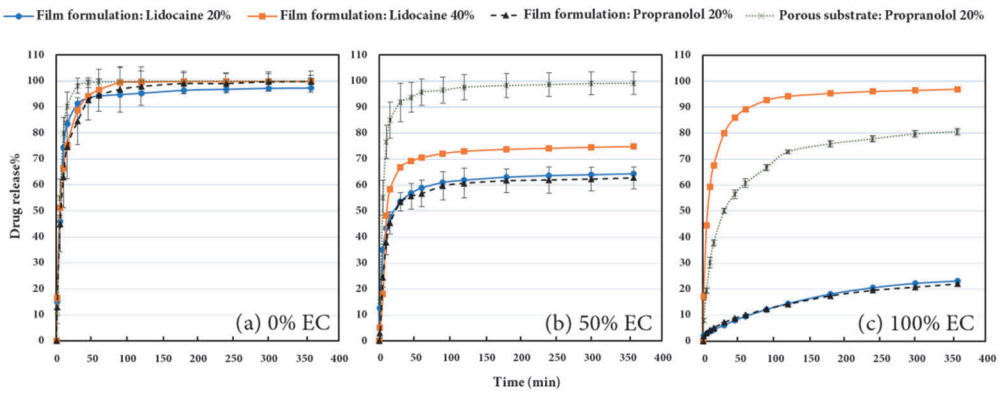

Figure 15. *Drug release profiles of all the formulations measured by the potentiometric technique (I). Data are presented as mean ± standard deviation (n = 3).*

The most noticeable feature in the release profiles was the fact that, as the concentration of EC increased, the drug release rate decreased accordingly for all the formulations with the most drastic results in case of 100% EC **(Figure 15 (a) – (c))**. The drug release was almost immediate in the absence of EC in the formulations. More than 80% of the drug was released in the first 20 min which resulted from high aqueous solubility and swelling of HPC in the dissolution medium (**Figure 15 (a)**). Also, the drug release from the porous cellulose substrate was much faster than the film formulations in each case. This was due to the more porous nature of this substrate, its larger surface area (Ø 28 mm compared to Ø 20 mm for the films) and the fact that the substrate structure prevented the complete formation of a polymer matrix which governed the release. The drug release from the film formulations was very similar for both drugs with the same concentration (20 w%) in identical polymer ratios **(Figure 15 (a) – (c))**. As the lidocaine concentration was raised from 20 w% to 40 w% in the drug-polymer blend, the drug release rates were also increased especially in case of 100% EC where the drug release was significantly faster **(Figure 15 (c))**. This great difference in drug release profiles could be related to the inability of EC without the HPC to entirely form a non-diffusible layer to control the drug release in case of 40 w% of the drug in the drug-polymer system.

For paper (II), the dissolution profiles of 2 APIs, propranolol hydrochloride and riboflavin sodium phosphate, from different formulations that were printed on 4 different substrates with multiple polymer coating (5 and 30 layers) were studied. The printed formulations were coated on both sides with a water impermeable polymeric membrane consisted of EC:ethanol (5:95 w%) using flexographic printing in order to investigate the effect of such polymer coatings on the drug release profiles. The thickness of each coating layer was calculated to be between 100 and 200 nm. The extensive dissolution results are presented in **Figure 16**.

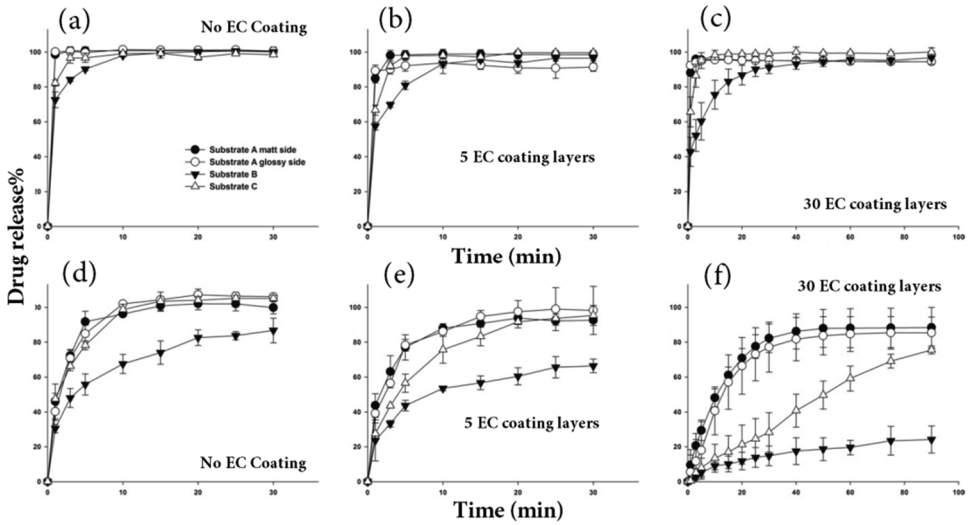

Figure 16. *Drug release profiles of propranolol hydrochloride (a–c) and riboflavin sodium phosphate (d–f) printed on different substrates: (a) and (d) without any coating; (b) and (e) after five layers of EC coating and coating (c) and (f) after 30 layers of EC coating (II). Data are presented as mean ± standard deviation (n = 3).*

Propranolol was almost completely released from all the uncoated formulations in the first 10 min **(Figure 16(a))**. Propranolol release from substrate 'B' was slightly affected in the early stages after EC coating; however, the drug release from the other substrates was not affected significantly after coating **(Figure 16(b) and (c))**. The riboflavin sodium phosphate release was observed to be slower than propranolol for each case. Both sides of substrate 'A' showed nearly identical release profiles for both drugs. The riboflavin release was generally more affected especially for substrates 'B' and 'C' after coating **(Figure 16 (d) – (f))**. The drug release from substrate 'B' was found to be the slowest which was followed by substrate 'C'. These two substrates were found to be better candidates for manufacturing controlled-release printed formulations coated by EC. The results showed the effect of the water impermeable coating together with the nature of substrates on the release of both APIs as the number of coating layers increased **(Figure 16(b), (c), (e) and (f))**.

According to Ozturk et al. (1990), the drug release through EC coated layers is a function of the thickness and the integrity of the coating material since diffusion through the film coating has been considered as one of the main driving forces for drug dissolution. The difference in the release behavior between the APIs was related to different solubility values of the APIs in ethanol which was used as the solvent in the coating polymer solution. Propranolol hydrochloride is soluble in ethanol but riboflavin sodium phosphate has poor solubility in ethanol (European pharmacopoeia, 2011). For this reason, it was speculated that propranolol could

partially dissolve and migrate into the forming polymeric layer during flexographic printing which later resulted in higher diffusion and subsequently higher dissolution rate of the drug from the formulations in the presence of the acidic dissolution medium. Swelling of the fibers of the substrates in contact with aqueous medium according to the nature, surface roughness and topography of these substrates could also cause partial detachment from polymeric coating layers and further explain the release behavior of the APIs from the substrates. Also, after cutting of each dosage form into single units, the sides of the edges were left exposed without coating which could be a helping factor for penetration of the dissolution media and eventually speeding up the dissolution process. It must be noted that the very thin layer of the coating which was less than 6 μm for 30 coating layers together with the abovementioned factors, resulted in faster drug release than reported by Ozturk et al. (1990) in which the EC coatings thickness varied between 9 and 50 μm.

In summary, it was confirmed that the presence of non-soluble EC polymer both within the formulations and as a coating layer could significantly govern the drug release of the printed and solvent-casted formulations.

5.5 Disintegration time and texture analysis (IV–V)

During disintegration studies for paper (IV), immediate swelling was observed for both ERP and CERP substrates when introduced to the aqueous medium (Phosphate buffer pH6). The disintegration mechanism of EIS was seen to be governed by the erosion of the particles from the surface of the substrate. The disintegration results are presented in **Table 1**. EPR showed the fastest disintegration time. The added HPC layer on CERP extended the disintegration time of this substrate more than twice as compared to ERP. The data clearly showed the influence of the clip weight in decreasing the disintegration time. However, as the clip weight increased, the change in disintegration time of EIS was not as considerable as it was for the other two substrates since its disintegration was governed by erosion. In conclusion, the disintegration time results were all within the defined 180 s (Ph.Eur.).

Table 1. *Disintegration time (s) of the substrates using different weights (g). Data are presented as mean ± standard deviation (n = 10).*

Clip weight (g)	ERP	CERP	EIS
3	20.04±1.99	43.58±5.24	69.34±5.21
5	11.99±1.52	36.86±4.43	64.10±5.62

The texture analysis and the disintegration results of the blank and the printed substrates for paper (V) are presented in **Table 2**. The disintegration times were well

within the limit of 180 s for both substrates before and after printing, even though the exerted force of 0.01 N (1 g clip weight) was lower than the approximate minimal force applied by the human tongue (0.03 N) (Hermes, 2012). PFS disintegrated much faster than EIS when introduced to the aqueous medium. Also, printing had only a slight effect to lower the disintegration time of both substrates.

Table 2. *Texture properties and disintegration values of the raw and the printed substrates. Data are presented as mean ± standard deviation (n = 10).*

	Tensile strength (N/mm^2)	Puncture resistance (kPa)	Distance at burst (mm)	Elongation %	Disintegration time (s)
Blank EIS	0.59±0.16	15.28±3.99	1.39±0.09	4.44±0.45	72.48±2.88
700 dpi on EIS	0.23±0.03	12.00±1.16	1.41±0.19	5.46±1.01	71.68±3.16
1000 dpi on EIS	0.17±0.04	8.97±0.47	1.35±0.2	5.25±0.94	71.56±3.28
Blank PFS	3.21±0.17	45.20±4.74	1.67±0.21	7.02±1.32	8.57±1.15
700 dpi on PFS	1.36±0.32	25.08±4.67	1.53±0.18	5.94±1.1	8.21±1.44
1000 dpi on PFS	1.69±0.21	19.83±4.46	1.18±0.24	5.85±0.85	7.58±1.75

In conclusion, as compared to the printed formulations, the blank substrates showed higher mechanical resistance towards the potential physical damage in the production line. This was more evident for PFS that was produced as a thin film manually. The disintegration time was reduced as the printing resolution increased; however, not significantly.

5.6 SC-ISEs and potentiometric technique (I)

For paper (I), the performance of the ion-selective electrodes that were designed and conditioned to be selective for propranolol hydrochloride was validated by comparison of the drug release profiles between the two methods of UV spectroscopy and potentiometry **(Figure 17)**.

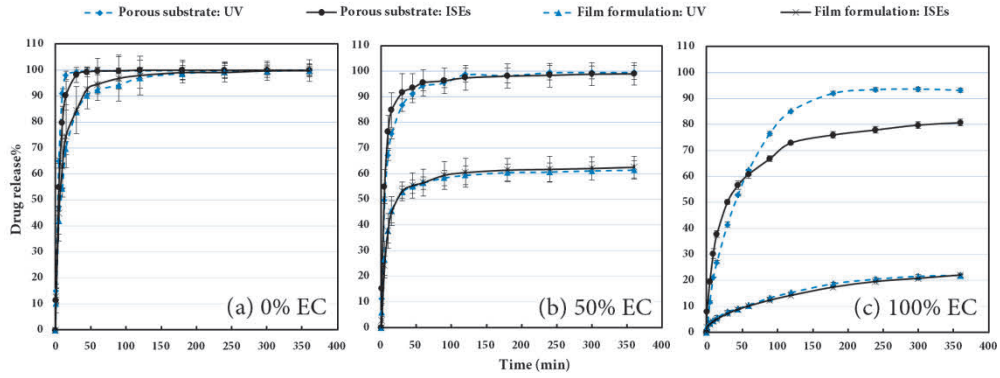

Figure 17. *Comparison of ion-selective electrodes (ISEs) to UV spectrophotometry in measurement of the drug release from the drop-casted film formulations (n = 3).*

The data showed almost identical drug release profiles in all formulations for both methods except in case of porous substrate in presence of only EC **(Figure 17 (c))**. In this case, after an hour mark a noticeable difference (<12% release) between the two profiles was observed. This difference was speculated to be the result of the interaction of the released protonated propranolol molecules with the components of the cellulose substrate in the solution. As a result of this, a less free protonated form of propranolol (lower activity of Pr^+) was available to be detected by the electrodes.

The calibration plots of the electrodes revealed the lower detection limit and the deviation from the ideal value of 59.16 mV in the slope of the curves for every 10−fold decrease in the concentration (cycle) of the APIs in the medium. The lower detection limit and the slope of the curves were found to be 0.92 μg/ml and 57.8 mV for propranolol selective electrodes and 0.54 μg/ml and 57.1 mV for lidocaine selective electrodes. Such values were considered quite satisfactory given the fact that the ideal slope for the working range of the ISEs is 59.16 mV per cycle. In addition, comparison of the lower detection limits of the propranolol electrodes to the UV spectroscopic instrument revealed a slightly lower detection limit for the electrodes (0.92 μg/ml) as the absorbance read value from a solution with the concentration of 1 μg/ml was already deviated from the linear relationship with the higher concentrations of the drug.

In conclusion, the ISEs showed promise as a fast-responding, inexpensive, accurate and reliable alternative for the study of the drug release from various formulations. In addition, potentiometric measurement was capable of collecting data in only a few seconds increment that resulted in more continuous monitoring of the drug release compared to the UV method. Further investigations were carried out to study the quality and working conditions of the electrodes.

5.7 Hyperspectral NIR imaging technique (III)

For paper (III), the entire escalating printed system was scanned by a hyperspectral imaging instrument. The spectral information was collected from each pixel in the field of view and then with the help of multivariate analysis was translated into the final concentration maps for readings of the API content from any desirable area. The PCA revealed that PC_1 and PC_2 explained 59.0% and 6.9% of the variations in the spectral data, respectively. In addition, the loading profile **(Figure 18)** of the first two principal components showed the most influential wavelength on the overall form of the scores plot. It is well known that variables with further distance from the neutral axis on the loading plot have a stronger impact on the model in opposite directions when situated above or below the neutral axis. Therefore, it was concluded that the spectral data related to the specific wavelengths of 1940 nm,

defined by PC_1, were responsible for explaining the most relevant variation in the entire data cloud.

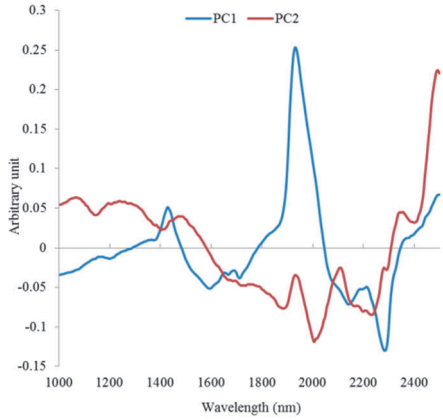

Figure 18. *The loading plots of the first and the second principal components.*

The pseudocolor RGB score image of the printed system **(Figure 19(a))** was then generated in which PC_1 was coded as red and PC_2 was coded as green. **Figure 19(a)** presents a spatial map that associates the spectral signatures to colors in RGB color space in order to distinguish regions with similar and contrasting chemical compositions. The number of printed layers and, therefore, the amount of deposited API increased continuously from the top left square unit to the bottom right one as it was also displayed in the pseudocolor RGB score image. Similarly, the PCA contour 2D plot **(Figure 19(b))** was created to demonstrate the spatial displacement of individual pixels according to their chemical composition. Each pixel was color coded in a continuum changing from cold (blue) to warm (red). It was evident that the increase in API content was in agreement with the shift from blue to red color. The score plot **(Figure 19(c))** which used the same color coding system represents the relationships between observations on a new coordinate system defined by the first two principal components.

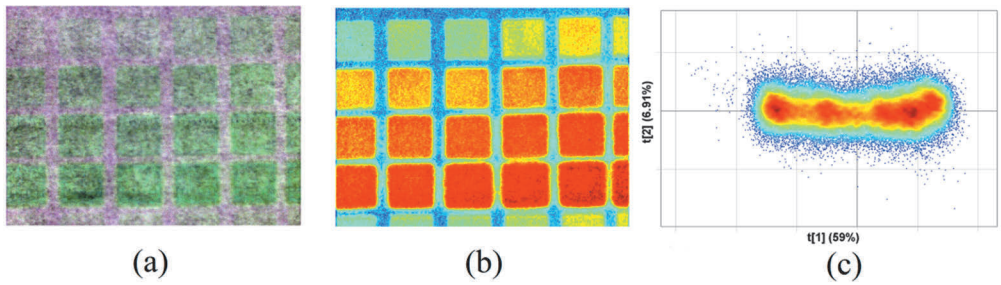

Figure 19. *Plots of hyperspectral imaging. (a) RGB image of the original set of formulations; (b) the PCA contour 2D plot and (c) the score plot.*

From an analytical point of view, the possibility of observing such detailed visual information that could be directly correlated to the drug amount is the indication of the great functionality of hyperspectral NIR imaging technique in quality control of the printed dosage forms.

Finally, the plot of predicted vs. measured API content is presented in **Figure 20**. The predicted values for samples with lower API content had greater error due to the interference of the substrate signal. Overall, the good correlation (R^2 = 0.974) between the predicted and measured values showed the high power of the created model for estimation of the drug amount in the formulations.

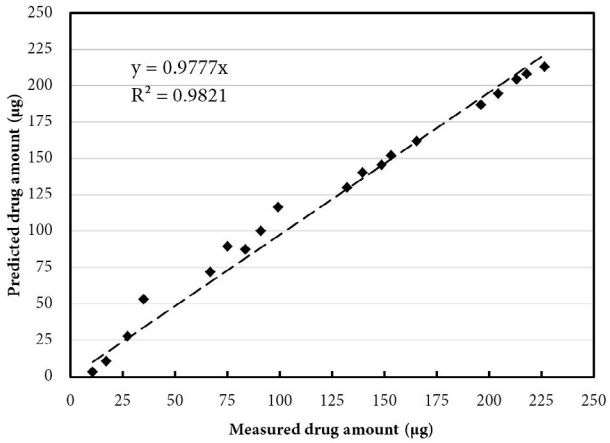

Figure 20. *The plot of predicted vs. measured API content.*

5.8 Colorimetric technique (IV)

In experiments related to paper (IV), the propranolol contained ink solution was naturally colorless. Therefore, for the purpose of conducting a colorimetric measurement it was required to add a coloring agent to the ink solution before printing. The assumption was made knowing that as long as both the API and the coloring agent were dissolved in a clear solution, their respective amounts would be identical in any portion of the ink solution. Thus, by measuring the color differences between the surface of the printed formulations and the reference surface, one could estimate the API amount indirectly. If that assumption were to be correct, then there would be a meaningful correlation between the colorimetric coefficients of the printed formulations and the number of printed layers. It is understood that the dose escalation in an inkjet printed system is always in great agreement with the number of printed layers. It should be noted that the comparison of ATR-IR spectra of the colored and non-colored API contained ink confirmed no chemical interactions between the coloring agent and the drug-excipients systems, which further justified the validity of the colorimetric measurements.

The colorimetric studies were performed in the CIELAB color space **(Figure 21(a))**. According to Eq. 3, it is known that each obtained numerical value of (ΔE*ab) is in fact *the distance* from the reference point in 3D CIELAB space. **Figure (21(b) – (d))** represent the 3D spatial location of (ΔE*ab) values of each individual printed unit on each substrate as a series of single data points on the chromaticity plots (the plane of a^* and b^*) with their corresponding lightness/intensity component (L^* axis) that was marked with the green lines. The total number of 3 substrates were used for this project and they were named as follows: edible rice paper (ERP), coated edible rice paper (CERP) and edible icing sheet (EIS).

A clear distinction between the color coordinates of the formulations was observed. For better visual understanding, one unit from each substrate (1 layer printed on ERP, 8 layers on CERP and 16 layers on EIS) was selected and their colorimetric components were highlighted in blue color **(Figure 21(b) – (d))**. As the number of printing layers increased, a systemic shift towards the red side of the chromatograms (right side) as well as an increase in the color intensity component were observed. This observation was confirmed for all the formulations, which further demonstrated the meaningful classification power of the applied colorimetric device.

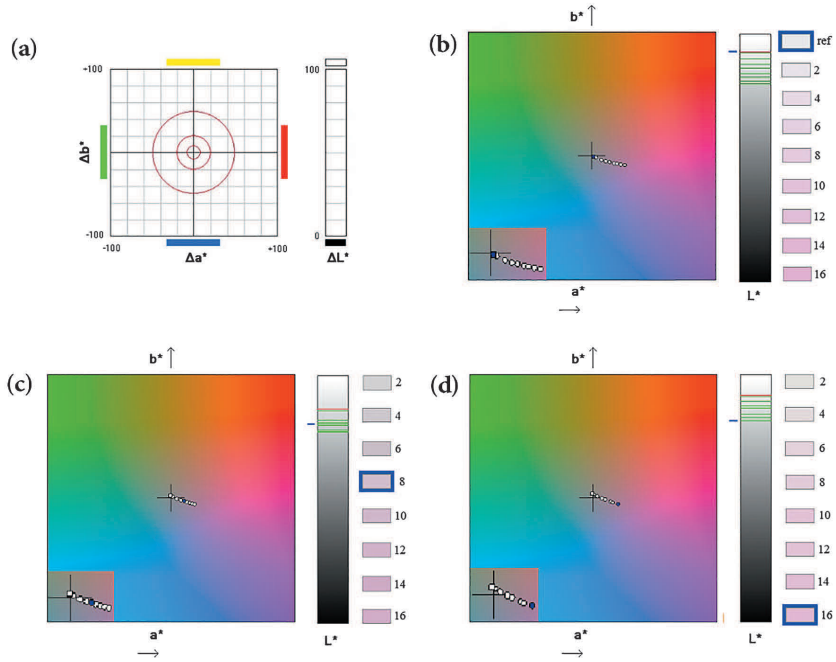

Figure 21. *(a) The CIELAB colorimetric system representing the numerical parameters a*, b* and L*; (b) chromaticity plot, lightness plot and generated color group of 2-16 layers of printed formulations on ERP substrate; (c) on CERP substrate and (d) on EIS substrate.*

Eventually, the validation of the colorimetric technique was accomplished by plotting (ΔE^*ab) values against the drug amount (mg) **(Figure 22)**.

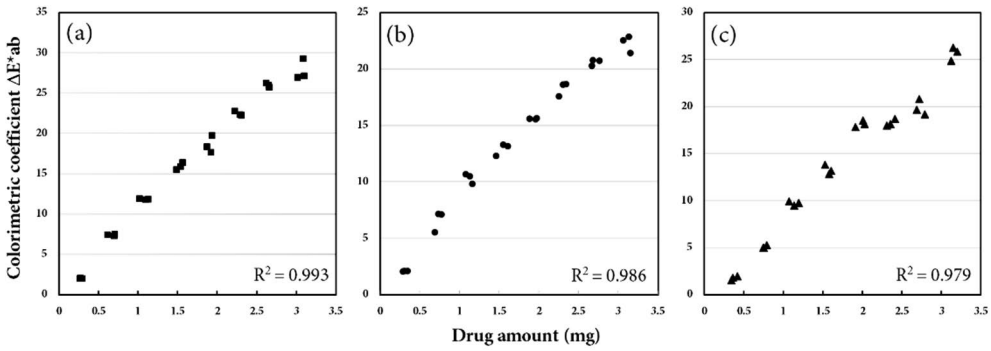

Figure 22. *Plots of colorimetric values ΔE*ab against the drug amount (mg) on 3 different substrates. (a) ERP; (b) CERP and (c) EIS.*

The fit accuracy (R^2) of the linear relationship between the ΔE^*ab values and the drug amount was found to be 0.993, 0.986 and 0.979 for ERP, CERP and EIS, respectively. The printing ink penetrated deeper inside the highly porous structure of ERP matrix and this resulted in more accurate color reading from the printed area with less deviation from the linearity compared to the other substrates. The shearing forces applied on the previously printed areas by the feeding rollers with the paper face-down feeding system affected the color uniformity of the less permeable and less absorptive EIS and CERP substrates. This is known as the smearing effect. As a result of this, there were more stained marks on these two substrates that were visible to the naked eye and possibly influenced the results.

The quality of the colorimetric technique was evident in the final results for all the substrates. It must be noted that the color difference values recorded in this study were due to the presence of the coloring agent in the ink solution and not the colorless drug. However, due to the linear relationship between the number of printed layers and the drug amount, as shown earlier in **(Figure 14(b)),** the color difference values could also be correlated to the drug content. The color of many inherently colorless drug containing ink solutions can be easily modified by the addition of inert coloring agents exclusively for the purpose of conducting colorimetric measurements. The applied colorimetric technique can be successfully calibrated and used as a fast and non-invasive quality control method for printed formulations. The presented approach is widely transferable when dealing with APIs that are freely soluble in the solvent with no risk of precipitation or degradation. Further investigation was carried out by ATR-IR spectroscopy to ensure that there was no chemical interaction between the drug and the excipients that could affect the results (reference to paper IV).

5.9 NIR measurements (V)

5.9.1 Model analysis

For paper (V), PCA and OPLS methods were performed on the collected spectra from dose escalating printed systems containing prednisolone and levothyroxine sodium in the range of 1550–1950 nm. The modelling parameters were obtained by cross–validation of the data in 7 groups as default **(Table 3)**.

Table 3. Summary of predictive models created by OPLS method.

Model	PC[a]	Filter summary	Q^2 (cum)	R^2Y (cum)	R^2x (predictive)	R^2x (cum)	RMSE*cv* (mg)	RMSEE (mg)
Prednisolone on EIS	1+1	Ctr-SG-3rd der	0.982	0.983	0.944	0.995	0.069	0.069
Prednisolone on PFS	1+1	Ctr-SG-3rd der	0.988	0.99	0.944	0.996	0.056	0.054
Levothyroxine on EIS	1+2	Ctr-SG-3rd der	0.958	0.962	0.926	0.995	0.051	0.050
Levothyroxine on PFS	1+2	Ctr-SG-3rd der	0.941	0.948	0.874	0.992	0.061	0.060

[a] R^2x (predictive) + number of R^2x_o (orthogonal).

The predictive ability (Q^2 (cum)) of the models was found to be in the range of 0.941–0.988 and the goodness of fit values (R^2Y (cum)) were in the range of 0.948–0.990. R^2x (predictive) values were between 87.4% and 94.4%, showing how well PC_1 could explain the variation in the data cloud in its direction. Furthermore, it could be seen that more than 99.2% of the variance in the X matrix was explained in all models with only 2 or 3 PCs indicating the low complexity of the datasets. Root mean square error of cross–validation (RMSE*cv*) and root mean square error of estimation (RMSEE) for the models show that only about 5% of the predicted concentration values would have an error of estimation more than ±0.07 mg in all the models.

5.9.2 Classification of observations

The OPLS scatter score plots of the models are illustrated in **Figure 23**. Scatter score plots are the projection of the multidimensional data cloud on the 2D plane with a new system of coordination (PCs) for better understanding and interpretation of the variations in the original datasets. The spectra of each single printed dosage form were translated into a single observation point on the score plot to disclose the interrelationship between the observations in each model. The plots indicated that the data carry class separating information and the OPLS methods were able to separate different classes of each model. The classification of the observations was more powerful for prednisolone models **(Figure 23(a) and (b))** in which no considerable overlap between neighboring class regions was observed as compared to levothyroxine models **(Figure 23(c) and (d))**.

The separation of classes in the t[1] direction demonstrated the variation *between* classes. The variation in this direction was the most important as R^2X [1] values revealed that between 87.4% and 94.4% of all the variations in each data clouds were in the direction of the first principal component. In other words, only one vector (PC_1) passing through the data cloud in each model could explain the most significant portion of all the variations in its direction. This finding was clearly in agreement with the design of experiment (DoE) in which the amount of deposited drug was the only factor defining the differences between the formulations. However, the separation in the t_o[1] direction was corresponding to the variations *within* classes which were caused mainly by the baseline shift in the spectra. The first orthogonal vector (R^2X_o[1]) in each model was only responsible for explaining between 4.40% and 8.35% of the remaining variations. This indicated the insignificance of the variations in this direction as compared to the R^2X [1] direction. Thus, the t_o[1] axis mostly served to generate and display the score plots in two-dimensions.

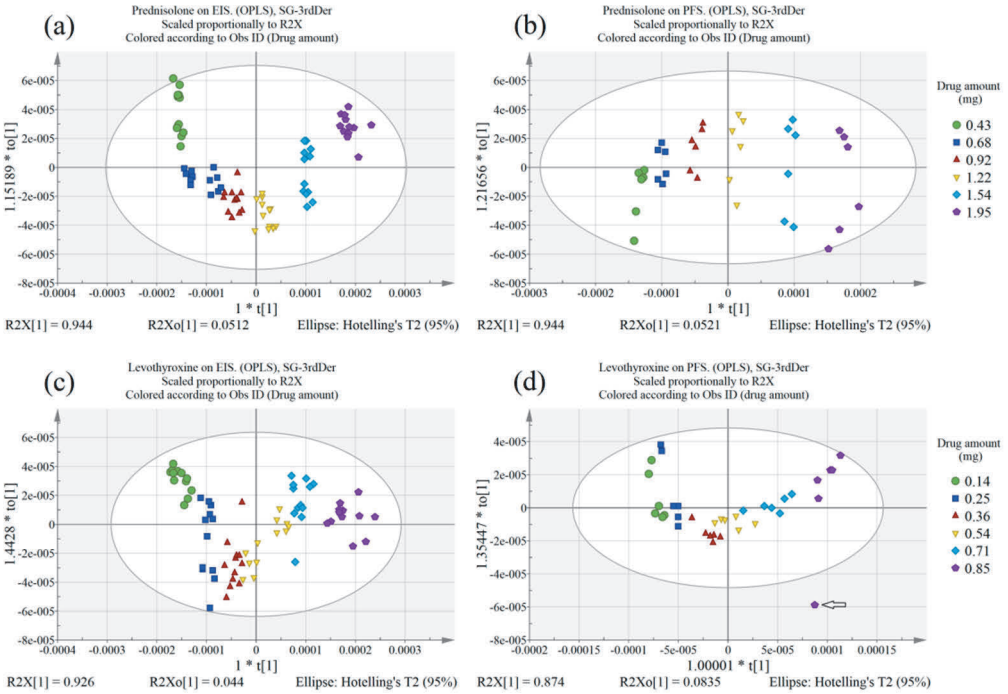

Figure 23. *Score scatter plots of the OPLS models scaled proportionally to R^2X. (a) prednisolone on EIS; (b) prednisolone on PFS; (c) levothyroxine on EIS and (d) levothyroxine on PFS. The observations are colored according to their respective drug amount.*

5.9.3. Predictions

The validation plots of the predictive models are presented in **Figure 24**.

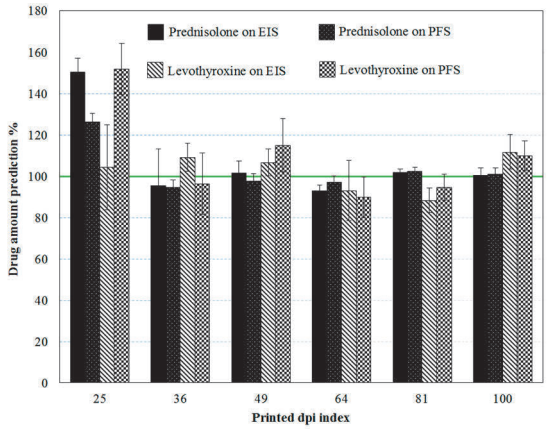

Figure 24. *The validation plots of the predictive models according to the print resolutions (dpi index) for both drugs. (n=10 for EIS and n=5 for PFS). The 100% line marks the actual drug amount that was measured by the reference analytical methods.*

The error of prediction was higher for the lowest doses, mainly due to the undesired effects of the spectral signals arising from the substrates (high noise-to-signal ratio). Since the prednisolone models had higher predicting power **(Table 1)**, they showed more accurate predictive qualities with lower standard deviations. The error variance (R^2) of the observed vs. predicted for prednisolone content was found to be 0.991 on EIS and 0.997 on PFS and for levothyroxine content R^2 was 0.952 on EIS and 0.968 on PFS when the highly erratic predictions of the lowest doses were not included.

In conclusion, such results show promise in applicability of the handheld NIR probe for on-site prediction of drug content of the printed formulations in a non–invasive fashion at the point of care.

5.10. DSC (IV–V)

Propranolol hydrochloride can exist in three crystalline forms, which are denoted as form I, II and III according to their decreasing melting points (Bartolomei et al., 1998). The DSC thermogram of the pure drug in **Figure 25 (a)** showed a sharp endothermic peak at 164.28 °C with heat of fusion (ΔH_f) of 134.2 J/g and onset temperature at 161.96 °C representing the melting point of the commercially available polymorph II of propranolol hydrochloride. The DSC thermogram of the freshly printed formulations did not feature any thermal events **(Figure 25(b), (c) and (d))**. After 3 months of storage time, thermograms of ERP and CERP formulations revealed weak endothermic thermal events with onset temperatures at

152.02 ˚C (ΔH_f = 7.55 J/g) and 144.33 ˚C (ΔH_f = 2.24 J/g), respectively **(Figure 25(e) and (f))**. These thermal events were indicative of a partial recrystallization of the drug in time. The onset temperatures of these melting peaks were shifted to lower temperatures due to the interactions of the drug with the potato starch. The presence of HPC polymer on CERP seemed to fairly reduce such interactions between the drug and the potato starch underneath. There was also no thermal event observed for the stored EIS formulations **(Figure 25(g))** much like all the fresh formulations which further indicated that the drug was molecularly dispersed within the substrate matrix.

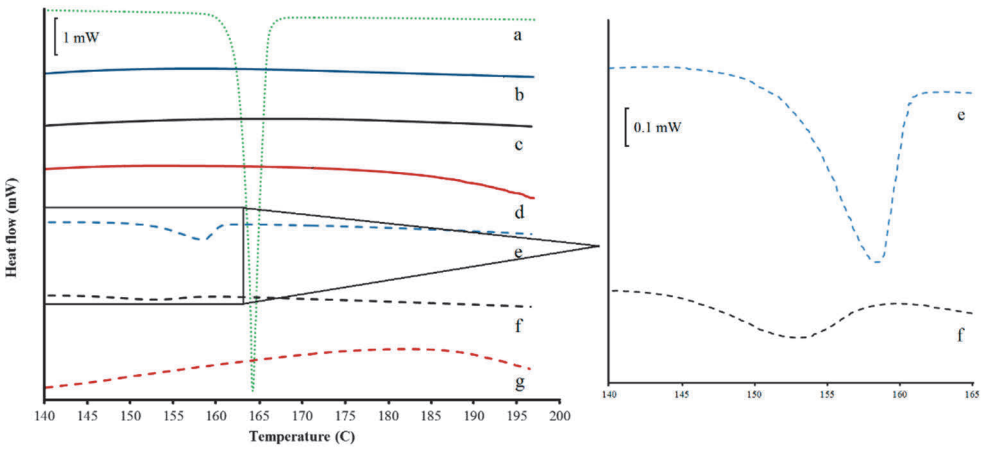

Figure 25. *DSC thermograms of (a) pure propranolol hydrochloride; (b) 16 layers on ERP; (c) 16 layers on CERP; (d) 16 layers on EIS; (e) 16 layers on ERP after 3 months; (f) 16 layers on CERP after 3 months and (g) 16 layers on EIS after 3 months.*

6. Conclusions

This thesis presents the very first step as comprehensive research with the focus on exploring the potential of various analytical techniques in quality control of printed pharmaceutical dosage forms. Performance of a series of compact, cost-effective and non-destructive analytical methods was investigated for real time monitoring of drug content uniformity and drug release profiles of printed formulation to provide further research advancements towards the goal of ultimate adoption and regulation of such techniques in the pharmaceutical industry. Various inkjet printing technologies were used to successfully manufacture dose flexible drug delivery systems in microgram precision. The printed formulations contained a variety of poorly water soluble drugs, narrow therapeutic index drugs and drugs that were prone to first-pass metabolism. Dose flexibility was achieved either by printing several superimposed layers or by changing the print resolution to adjust the number of drops in a defined area size. The drug amounts on printed formulations have repeatedly proved to be highly linear with respect to escalation of printing layers or resolution. Therefore, in agreement with many publications on the subject, it was concluded that inkjet printing was an extremely accurate method for rapid and on-demand deposition of various APIs on planar substrates. Also, the control over the drug release profiles of the manufactured formulations was effectively accomplished either by addition of the polymers directly with the drug in the formulation design or by several layers of additional polymeric coating on already printed formulations by flexographic printing or manually with a coating knife.

In the future, when inkjet printing is eventually authorized for printing pharmaceuticals, there will be a demand for production of specific inkjet printers with simpler, more affordable and more compact design using disposable units to help resolving practical issues such as cleaning of tubing and the printhead after each printing job in order to avoid clogging, contamination and waste of time and materials.

The surface morphology and visual microscopy were also conducted in various studies to gain a deeper understanding about the effect of printing on the substrate and the physical changes in microscopic levels. The solid-state properties of the formulations were examined using differential scanning calorimetry and attenuated total reflection infrared which revealed that in many cases the drugs were molecularly dispersed within the porous structure of the substrates as no significant chemical reaction between the drug and excipient was recorded. Additional mechanical, texture and disintegration analyses were carried out to ensure the

physical properties of the orodispersible formulations within the latest framework defined by Ph. Eur.

Ion-selective electrodes that were designed to be responsive for two drugs showed good quality under various conditions and were able to reliably measure the drug release in steps of a few seconds from porous cellulose matrices. NIR hyperspectral imaging was used to predict the drug amount and to create highly informative concentration distribution maps of the drug in printed formulations in a non-destructive manner. The application of a handheld colorimetric device in CIELAB color space showed promise in the assessment of the drug content simply by measuring the color difference values of the dose escalating system of formulations. Such encouraging results of the colorimetric technique suggested a broad range of possibilities for addition of inert coloring agents to various colorless ink solution and the subsequent indirect estimation of the drug in the printed formulations. Finally, a compact handheld probe was used to collect the NIR spectra from the surface of the printed formulations. The spectra were subsequently treated using sophisticated chemometrics for interpretation of the multivariate data and building the predictive models. This NIR device has never been used in pharmaceutical research before and it proved to have the potential for in-line, non-invasive and reliable quality control of the printed formulations at the envisaged point of care manufacturing scenario.

In the end, additional research is necessary to focus on many remaining issues such as the interaction of various drug candidates with many possible printing inks and substrates, the effect of drug degradation and solid-state transformation in presence of various excipients for each scenario, the stability of the drug in the printing ink, the effective removal of the organic ink solvents from the printed formulations, finding optimal printing parameters suitable for different inks and printers, deeper understanding of the possible sources of error and interference in each analytical practice and further exercise on handling the chemometrics to maximize the useful information in the obtained multivariate data.

7. Sammanfattning (Summary in Swedish)

Det finns ett behov av utveckling och produktion av farmaceutiska dosformer med flexibel dosering för att uppnå de centrala kraven för precisionsmedicin för patientspecifik terapi. Precisionsmedicin innebär ett paradigmskifte i klinisk praxis, personifierad diagnostisering av sjukdomen, individuell formuleringsdesign och tillverkning av skräddarsydda doseringsformer för att åstadkomma en optimal och väl tolererad terapeutisk behandling.

Nya teknologier möjliggör vid behov tillverkning av små läkemedelssatser med dosflexibilitet. Detta är viktigt i framställning av skräddarsydda läkemedel nära patienten, till exempel i sjukhus eller på apotek. I detta avseende har bläckstråleutskriftsteknik föreslagits under det senaste decenniet som en metod att deponera extremt noggranna och små mängder läkemedel på olika ätbara polymerfilmer. Dagens bläckstråleskrivare med kompakt design, öppen arkitektur och avancerade integrerade visualiseringssystem erbjuder noggrann kontroll över storleken och placeringen av de tusentals enskilda bläckdropparna i picolitervolym. Utskrivna läkemedel formuleras ofta på ett sätt att de upplöses snabbt i munnen vilket underlättar administrering och ger en högre följsamhet av behandlingen, speciellt för barn och personer med sväljningssvårigheter. Ifall läkemedlet absorberas genom munslemhinnan direkt till den systemiska cirkulation kan förstapassagemetabolismen i levern också undvikas vilket kan leda till en snabbare terapeutisk effekt.

En av de viktigaste aspekterna för att tillsynsmyndigheterna ska acceptera bläckstråleskrivning som en allmänt accepterad metod för kontinuerlig tillverkning, krävs snabba, robusta, pålitliga och icke-invasiva analytiska metoder för kvalitetskontroll. Denna avhandling var huvudsakligen inriktad på att utforska olika analytiska metoder och småskaliga instrument för att studera doseringsnoggranhet och läkemedelsfrisättning i de tryckta läkemedelsformuleringarna.

Jonselektiva elektroder konstruerades för kontinuerlig övervakning av läkemedelsfrisättningen från porösa cellulosasubstrat och tunna filmer som ett försök att föreslå ett kostnadseffektivt och effektivt alternativ till konventionella tids- och arbetskrävande metoder. Flexografisk tryckteknik utnyttjades för att applicera flera lager av högviskös och olöslig polymerbeläggning på redan bläckstråleskrivna formuleringar för att uppnå formuleringar med modifierade frisättningsprofiler. Närainfraröd hyperspektral bildbehandling tillämpades för att förutsäga läkemedelsmängden och att skapa koncentrationsfördelningskartor som erbjuder både statistiska och visuella bedömningar av de tryckta formuleringarna. Användningen av en kompakt kolorimetrisk apparat undersöktes (i CIELAB

färgutrymme) för att uppskatta läkemedelsinnehållet i pediatriska munsönderfallande formuleringar. Slutligen användes en NIR-spektrometer i miniatyrform tillsammans med avancerade kemometriska metoder för att bygga prediktiva modeller för att analysera läkemedelsinnehållet i doseringsformerna. Dessutom behandlas tillämpningen av multivariata dataanalysstekniker för bearbetning och modellering av spektroskopiska data i detalj. Flera andra analytiska tekniker användes även för att studera ytmorfologi, ythårdhet, ytstruktur, mekaniska egenskaper och fasta fasens egenskaper hos de obehandlade och tryckta substraten samt stabiliteten av formuleringarna. Fördelarna och bristerna av varje formuleringsdesign och tillämpad analysmetod lyfts fram och en allmän strategi för framtida studier föreslås.

Denna forskning ger en djupare inblick i bläckstråleskrivningsprocessen för läkemedelsformuleringar och ger ny förståelse om användbarheten av olika icke-invasiva kvalitetskontrollsverktyg i tillverkning av personifierade läkemedelsformer.

8. Acknowledgments

This thesis is based on the research that was carried out at the Pharmaceutical Sciences Laboratory, Faculty of Science and Engineering, Åbo Akademi University, during the years 2012-2017.

The research was supported by Tekes, the Academy of Finland, Finnish Cultural Foundation and Doctoral Education Network in Materials Research (DNMR) of Åbo Akademi University.

I would like to express my deepest gratitude and sincere respect to my primary supervisor Professor Niklas Sandler for his endless help, exceptional leadership and incredibly wonderful attitude on every day of every week and regarding all matters which altogether made it possible for me to continue working throughout many hard phases in the past years to complete this journey. Mere words cannot simply do the justice, Sir. In addition, I would like to thank Professor Johan Bobacka who patiently and masterfully guided me during my Master's studies and also during the early stages of my PhD research.

I am sincerely thankful to Dr. Natalja Genina, as she educated and guided me about many fundamental levels of knowledge in the pharmaceutical field in the first two years of my research. Also, many thanks to post-doctoral researchers, Dr. Ruzica Kolakovic who helped me through my third publication always with a smile as well as Dr. Maren Preis for constructive instructions during later stages of my research.

I am deeply grateful to have Professor Clare J. Strachan from University of Helsinki, Finland and Professor Maike Windberg from Goethe University, Germany as reviewers of this thesis. Their valued opinions further strengthened my self-confidence regarding the quality of my research.

I would like to acknowledge all of co-authors and co-workers at Åbo Akademi University for their help and contribution during various stages of this research work. Moreover, I am pleased with all of my colleagues, Emrah Yildir, Henrika Wickström, Heidi Öblom, Mirja Palo, Erica Sjöholm and many other research visitors who naturally became friends and contributed to a productive work environment throughout these years. Additional credit to my beautiful girlfriend Alicja Drynkowska who stood by me and helped me keep the balance in my personal life.

Finally, I am eternally grateful for the infinite spiritual support of my family, my beloved sister and above all my mother who made life possible for me on this plane of existence.

Åbo, 2018
Hossein Vakili

9. References

Aboul-Enein, H.Y., Sun, X.X. (2000). A novel PVC membrane electrode for determination of propranolol in pharmaceutical formulation. *Analusis*, 28 (9), 855–858.

Alexandrino, G.L., Poppi, R.J. (2013). NIR imaging spectroscopy for quantification of constituents in polymers thin films loaded with paracetamol. *Analytica Chimica Acta*, 765, 37–44.

Alomari, M., Mohamed, F.H., Basit, A.W., Gaisford, S. (2015). Personalised dosing: Printing a dose of one's own medicine. *International Journal of Pharmaceutics*, 494 (2), 568–577.

Amigo, J.M., Ravn, C. (2009). Direct quantification and distribution assessment of major and minor components in pharmaceutical tablets by NIR-chemical imaging. *European Journal of Pharmaceutical Sciences*, 37 (2), 76–82.

Ansorena, D., Peña, M.P. de, Astiasarán, I., Bello, J. (1997). Colour evaluation of chorizo de Pamplona, a Spanish dry fermented sausage: Comparison between the CIE L(∗)a(∗)b(∗) and the Hunter lab systems with illuminants D65 and C. *Meat Science*, 46 (4), 313–318.

Bakker, E., Bühlmann, P., Pretsch, E. (1997). Carrier-Based Ion-Selective Electrodes and Bulk Optodes. 1. General Characteristics. *Chemical Reviews*, 97 (8), 3083–3132.

Barnes, R.J., Dhanoa, M.S., Lister, S.J. (1989). Standard Normal Variate Transformation and De-trending of Near-Infrared Diffuse Reflectance Spectra. *Applied Spectroscopy*, 43 (5), 772–777.

Bobacka, J. (1999). Potential Stability of All-Solid-State Ion-Selective Electrodes Using Conducting Polymers as Ion-to-Electron Transducers. *Analytical chemistry*, 71 (21), 4932–4937.

Bobacka, J., Ivaska, A., Lewenstam, A. (2008). Potentiometric ion sensors. *Chemical Reviews*, 108 (2), 329–351.

Borges, A.F., Silva, C., Coelho, J.F.J., Simoes, S. (2015). Oral films: Current status and future perspectives: I - Galenical development and quality attributes. *Journal of Controlled Release*, 206, 1–19.

Breitkreutz, J., Boos, J. (2007). Paediatric and geriatric drug delivery. *Expert Opinion on Drug Delivery,* 4 (1), 37–45.

Brniak, W., Maslak, E., Jachowicz, R. (2015). Orodispersible films and tablets with prednisolone microparticles. *European Journal of Pharmaceutical Sciences*, 75, 81–90.

Buanz, A.B.M., Saunders, M.H., Basit, A.W., Gaisford, S. (2011). Preparation of personalized-dose salbutamol sulphate oral films with thermal ink-jet printing. *Pharmaceutical Research*, 28 (10), 2386–2392.

Buck, R.P., Lindner, E. (1994). Recommendations for nomenclature of ionselective electrodes (IUPAC Recommendations 1994). *Pure and Applied Chemistry*, 66 (12). 2527–2536.

Bühlmann, P., Pretsch, E., Bakker, E. (1998). Carrier-Based Ion-Selective Electrodes and Bulk Optodes. 2. Ionophores for Potentiometric and Optical Sensors. *Chemical Reviews*, 98 (4), 1593–1688.

Calvo, C., Salvador, A., Fiszman, S. (2001). Influence of colour intensity on the perception of colour and sweetness in various fruit-flavoured yoghurts. *European Food Research and Technology*, 213 (2), 99–103.

Cheow, W.S., Kiew, T.Y., Hadinoto, K. (2015). Combining inkjet printing and amorphous nanonization to prepare personalized dosage forms of poorly-soluble drugs. *European Journal of Pharmaceutics and Biopharmaceutics*, 96, 314–321.

Clarke, A., Brewer, F., Johnson, E.S., Mallard, N., Hartig, F., Taylor, S., Corn, T.H. (2003). A new formulation of selegiline: improved bioavailability and selectivity for MAO-B inhibition. *Journal of Neural Transmission*, 110 (11), 1241–1255.

Collier, J.W., Shah, R.B., Gupta, A., Sayeed, V., Habib, M.J., Khan, M.A. (2010). Influence of formulation and processing factors on stability of levothyroxine sodium pentahydrate. *AAPS PharmSciTech*, 11 (2), 818–825.

Daly, R., Harrington, T.S., Martin, G.D., Hutchings, I.M. (2015). Inkjet printing for pharmaceutics - A review of research and manufacturing. *International Journal of Pharmaceutics*, 494 (2), 554–567.

Derby, B. (2010). Inkjet Printing of Functional and Structural Materials: Fluid Property Requirements, Feature Stability, and Resolution. *Annual Review of Materials Research*, 40 (1), 395–414.

Di Wu, Sun, D.-W. (2013). Colour measurements by computer vision for food quality control – A review. *Trends in Food Science & Technology*, 29 (1), 5–20.

Dixit, R.P., Puthli, S.P., 2009. Oral strip technology: overview and future potential. *Journal of Controlled Release*, 139 (2), 94–107.

Edinger, M., Bar-Shalom, D., Rantanen, J., Genina, N. (2017). Visualization and Non-Destructive Quantification of Inkjet-Printed Pharmaceuticals on Different Substrates Using Raman Spectroscopy and Raman Chemical Imaging. *Pharmaceutical Research*, 34 (5), 1023–1036.

Ely, D.R., Carvajal, M.T. (2011). Determination of the scale of segregation of low dose tablets using hyperspectral imaging. *International Journal of Pharmaceutics*, 414 (1-2), 157–160.

Eriksson, L., Byrne, T., Johansson, E., Trygg, J., Vikström, C. (2013). Multi- and Megavariate Data Analysis Basic Principles and Applications. 3rd ed. *MKS Umetrics AB*, Malmö, Sweden.

European Pharmacopoeia (2011). Propranolol hydrochloride. *7th ed*. Strasbourg: Council of Europe. 2811–2812.

European Pharmacopoeia (2011). Riboflavin sodium phosphate. *7th ed*. Strasbourg: Council of Europe. 2853–2854.

Food and Drug Administration (2004). Guidance for Industry PAT — A Framework for Innovative Pharmaceutical Development, Manufacturing, and Quality Assurance. Available from: https://www.fda.gov/downloads/drugs/guidances/ucm070305.pdf (20.06.2017).

Food and Drug Administration (2013). Paving the Way for Personalized Medicine—FDA's Role in a New Era of Medical Product Development. Available from: https://www.fda.gov/downloads/scienceresearch/specialtopics/personalizedmedicine/ucm372421.pdf (13.04.2017).

Franca, L.d.M., Pimentel, M.F., Simoes, S.d.S., Grangeiro, S., JR, Prats-Montalban, J.M., Ferrer, A. (2016). NIR hyperspectral imaging to evaluate degradation in captopril commercial tablets. *European Journal of Pharmaceutics and Biopharmaceutics*,104, 180–188.

Garsuch, V., Breitkreutz, J. (2010). Comparative investigations on different polymers for the preparation of fast-dissolving oral films. *The Journal of Pharmacy and Pharmacology*, 62 (4), 539–545.

Gendre, C., Boiret, M., Genty, M., Chaminade, P., Pean, J.M. (2011). Real-time predictions of drug release and end point detection of a coating operation by in-line near infrared measurements. *International Journal of Pharmaceutics*, 421 (2), 237–243.

Genina, N., Fors, D., Vakili, H., Ihalainen, P., Pohjala, L., Ehlers, H., Kassamakov, I., Haeggstrom, E., Vuorela, P., Peltonen, J., Sandler, N., 2012. Tailoring controlled-release oral dosage forms by combining inkjet and flexographic printing techniques. *European Journal of Pharmaceutical Sciences*, 47 (3), 615–623.

Genina, N., Fors, D., Palo, M., Peltonen, J., Sandler, N. (2013a). Behavior of printable formulations of loperamide and caffeine on different substrates--effect of print density in inkjet printing. *International Journal of Pharmaceutics*, 453 (2), 488–497.

Genina, N., Janssen, E.M., Breitenbach, A., Breitkreutz, J., Sandler, N. (2013b). Evaluation of different substrates for inkjet printing of rasagiline mesylate. *European Journal of Pharmaceutics and Biopharmaceutics*, 85, 1075–1083.

Giahi, M., Mirzaei, M., Veghar Lahijani, G. (2010). Potentiometric PVC membrane sensor for the determination of phenylephrine hydrochloride in some pharmaceutical products. *Journal of the Iranian Chemical Society*, 7 (2), 333–338.

Gu, Y., Chen, X., Lee, J.-H., Monteiro, D.A., Wang, H., Lee, W.Y. (2012). Inkjet printed antibiotic- and calcium-eluting bioresorbable nanocomposite micropatterns for orthopedic implants. *Acta Biomaterialia*, 8 (1), 424–431.

Hetrick, E.M., Vannoy, J., Montgomery, L.L., Pack, B.W. (2013). Integrating tristimulus colorimetry into pharmaceutical development for color selection and physical appearance control: a quality-by-design approach. *Journal of Pharmaceutical Sciences*, 102 (8), 2608–2621.

Hirshfield, L., Giridhar, A., Taylor, L.S., Harris, M.T., Reklaitis, G.V. (2014). Dropwise additive manufacturing of pharmaceutical products for solvent-based dosage forms. *Journal of Pharmaceutical Sciences*, 103 (2), 496–506.

Hoffmann, E.M., Breitenbach, A., Breitkreutz, J. (2011). Advances in orodispersible films for drug delivery. *Expert Opinion on Drug Delivery*, 8 (3), 299–316.

Homayoun, S.B., Shrikant, I.B., Kazem, M., Hemmat, M., Reza, M. (2011). Compared application of the new OPLS-DA statistical model versus partial least squares regression to manage large numbers of variables in an injury case-control study. *Scientific Research and Essays*, 6 (20), 4369–4377.

Hutchings, I.M., Martin, G.D. (2012). Inkjet technology for digital fabrication. *1st ed. Wiley*, West Sussex, United Kingdom.

Hölzl, K., Lin, S., Tytgat, L., van Vlierberghe, S., Gu, L., Ovsianikov, A. (2016): Bioink properties before, during and after 3D bioprinting. *Biofabrication*, 8 (3), 032002–1–19.

Ihalainen, P., Määttänen, A., Sandler, N. (2015). Printing technologies for biomolecule and cell-based applications. *International Journal of Pharmaceutics*, 494 (2), 585–592.

Irfan, M., Rabel, S., Bukhtar, Q., Qadir, M.I., Jabeen, F., Khan, A. (2016). Orally disintegrating films: A modern expansion in drug delivery system. *Saudi Pharmaceutical Journal*, 24 (5), 537–546.

Jain, K.K. (2002). Personalized medicine. *Current Opinion in Molecular Therapeutics*, 4 (6), 548–558.

Janssen, E.M., Schliephacke, R., Breitenbach, A., Breitkreutz, J. (2013). Drug-printing by flexographic printing technology--a new manufacturing process for orodispersible films. *International Journal of Pharmaceutics*, 441 (1-2), 818–825.

Jolliffe, I.T., Cadima, J. (2016). Principal component analysis: a review and recent developments. *Philosophical Transactions: Mathematical, Physical and Engineering Sciences*, 374 (2065), 20150202.

Karande, A.D., Heng, P.W.S., Liew, C.V. (2010). In-line quantification of micronized drug and excipients in tablets by near infrared (NIR) spectroscopy: Real time monitoring of tabletting process. *International journal of pharmaceutics*, 396 (1-2), 63–74.

Kays, S.J. (1999). Preharvest factors affecting appearance. *Postharvest Biology and Technology*, 15 (3), 233–247.

Khalil, S., Borham, N. (1999). Phenothiazine Drug Poly(vinyl chloride) Matrix Membrane Electrodes and Their Use in Pharmaceutical Analysis. *Microchemical Journal*, 63 (3), 389–397.

Kolakovic, R. (2013a). Nanofibrillar cellulose in drug delivery, *Doctoral thesis*, Helsinki, Finland, 60 pp.

Kolakovic, R., Viitala, T., Ihalainen, P., Genina, N., Peltonen, J., Sandler, N. (2013b): Printing technologies in fabrication of drug delivery systems. *Expert opinion on drug delivery*, 10 (12), 1711–1723.

Korasa, K., Hudovornik, G., Vrecer, F. (2016). Applicability of near-infrared spectroscopy in the monitoring of film coating and curing process of the prolonged release coated pellets. *European Journal of Pharmaceutical Sciences*, 93, 484–492.

Korifi, R., Le Dréau, Y., Antinelli, J.F., Valls, R., Dupuy, N. (2013). CIEL*a*b* color space predictive models for colorimetry devices--analysis of perfume quality. *Talanta*, 104, 58–66.

Kuscer, D., Stavber, G., Trefalt, G., Kosec, M., Brennecka, G. (2012). Formulation of an aqueous titania suspension and its patterning with ink-jet printing technology. *Journal of the American Ceramic Society*, 95 (2), 487–493.

Lai, C.Z., Fierke, M.A., Stein, A., Bühlmann, P. (2007). Ion-selective electrodes with three-dimensionally ordered macroporous carbon as the solid contact. *Analytical Chemistry*, 79 (12), 4621–4626.

Langreth, R., Waldholz, M. (1999). New era of personalized medicine: targeting drugs for each unique genetic profile. *The Oncologist*, 4 (5), 426–427.

Lau, E.T.L., Steadman, K.J., Mak, M., Cichero, J.A.Y., Nissen, L.M. (2015). Prevalence of swallowing difficulties and medication modification in customers of community pharmacists. *Journal of Pharmacy Practice and Research*, 45 (1), 18–23.

Laukamp, E.J., Thommes, M., Breitkreutz, J. (2014). Hot-melt extruded drug-loaded rods: evaluation of the mechanical properties for individual dosing via the Solid Dosage Pen. *International Journal of Pharmaceutics*, 475 (1-2), 344–350.

Le, H.P. (1998). Progress and threns in ink-jet printing technology. *Journal of Imaging Science and Technology*, 42 (1), 49–62.

Lee, B.K., Yun, Y.H., Choi, J.S., Choi, Y.C., Kim, J.D., Cho, Y.W. (2012). Fabrication of drug-loaded polymer microparticles with arbitrary geometries using a piezoelectric inkjet printing system. *International Journal of Pharmaceutics*, 427 (2), 305–310.

Linden, M. (2012). Influence of the formulation and extrusion process on extended- and enteric release profile. *Doctoral thesis*, Gothenburg, Sweden, 57 pp.

Low, A., Kok, S.L., Khong, Y., Chan, S.Y., Gokhale, R. (2015). Pharmaceutics, Drug Delivery and Pharmaceutical Technology: A New Test Unit for Disintegration End-Point Determination of Orodispersible Films. *Journal of Pharmaceutical Sciences*, 104 (11), 3893–3903.

Mallal, S., Nolan, D., Witt, C., Masel, G., Martin, A.M., Moore, C., Sayer, D., Castley, A., Mamotte, C., Maxwell, D., James, I., Christiansen, F.T. (2002). Association between presence of HLA-B*5701, HLA-DR7, and HLA-DQ3 and hypersensitivity to HIV-1 reverse-transcriptase inhibitor abacavir. *The Lancet*, 359 (9308), 727–732.

Mattinen, U., Bobacka, J., Lewenstam, A. (2009). Solid-Contact Reference Electrodes Based on Lipophilic Salts. *Electroanalysis*, 21 (17-18), 1955–1960.

Mattinen, U., Rabiej, S., Lewenstam, A., Bobacka, J. (2011). Impedance study of the ion-to-electron transduction process for carbon cloth as solid-contact material in potentiometric ion sensors. *Electrochimica Acta*, 56 (28), 10683–10687.

McDevitt, J.T., Gurst, A.H., Chen, Y. (1998). Accuracy of tablet splitting. *Pharmacotherapy*, 18 (1), 193–197.

McKinley, G.H., Renardy, M. (2011). Wolfgang von Ohnesorge. *Physics of Fluids*, 23 (12), 127101.

Melendez, P.A., Kane, K.M., Ashvar, C.S., Albrecht, M., Smith, P.A. (2008). Thermal inkjet application in the preparation of oral dosage forms: dispensing of prednisolone solutions and polymorphic characterization by solid-state spectroscopic techniques. *Journal of Pharmaceutical Sciences*, 97 (7), 2619–2636.

Meléndez-Martínez, A.J., Vicario, I.M., Heredia, F.J., 2003. Application of tristimulus colorimetry to estimate the carotenoids content in ultrafrozen orange juices. *Journal of Agricultural and Food Chemistry*, 51 (25), 7266–7270.

Meléndez-Martínez, A.J., Vicario, I.M., Heredia, F.J. (2005). Instrumental measurement of orange juice colour: A review. *Journal of the Science of Food and Agriculture*, 85 (6), 894–901.

Mogalicherla, A.K., Lee, S., Pfeifer, P., Dittmeyer, R. (2014). Drop-on-demand inkjet printing of alumina nanoparticles in rectangular microchannels. *Microfluid Nanofluid*, 16 (4), 655–666.

Montenegro-Nicolini, M., Miranda, V., Morales, J.O. (2017). Inkjet Printing of Proteins: an Experimental Approach. *The AAPS Journal*, 19 (1), 234–243.

Nilausen, D.Ø., Zuiker, R., van Gerven, J. (2011). The Perception and Pharmacokinetics of a 20-mg Dose of Escitalopram Orodispersible Tablets in a Relative Bioavailability Study in Healthy Men. *Clinical Therapeutics*, 33 (10), 1492–1502.

Novelli, G. (2010). Personalized genomic medicine. *Internal and Emergency Medicine*, 5 (1), 81-90.

Ozturk, A.G., Ozturk, S.S., Palsson, B.O., Wheatley, T.A., Dressman, J.B. (1990). Mechanism of release from pellets coated with an ethylcellulose-based film. *Journal of Controlled Release*, 14 (3), 203–213.

Palo, M., Kogermann, K., Laidmae, I., Meos, A., Preis, M., Heinamaki, J., Sandler, N. (2017). Development of Oromucosal Dosage Forms by Combining Electrospinning and Inkjet Printing. *Molecular Pharmaceutics*, 14 (3), 808–820.

Pardeike, J., Strohmeier, D.M., Schrodl, N., Voura, C., Gruber, M., Khinast, J.G., Zimmer, A. (2011). Nanosuspensions as advanced printing ink for accurate dosing of poorly soluble drugs in personalized medicines. *International Journal of Pharmaceutics*, 420 (1), 93–100.

Pavurala, N., Xu, X., Krishnaiah, Y.S.R. (2017). Hyperspectral imaging using near infrared spectroscopy to monitor coat thickness uniformity in the manufacture of a transdermal drug delivery system. *International Journal of Pharmaceutics*, 523 (1), 281–290.

Peh, K.K., Wong, C.F. (1999). Polymeric films as vehicle for buccal delivery: swelling, mechanical, and bioadhesive properties. *Journal of Pharmacy & Pharmaceutical sciences*, 2 (2), 53–61.

Planchette, C., Pichler, H., Wimmer-Teubenbacher, M., Gruber, M., Gruber-Woelfler, H., Mohr, S., Tetyczka, C., Hsiao, W.-K., Paudel, A., Roblegg, E., Khinast, J. (2016). Printing medicines as orodispersible dosage forms: Effect of substrate on the printed micro-structure. *International Journal of Pharmaceutics*, 509 (1-2), 518–527.

Preis, M. (2014). Oromucosal film preparations for pharmaceutical use – formulation development and analytical characterization, *Doctoral thesis*, Dusseldorf, Germany, 74 pp.

Preis, M., Breitkreutz, J., Sandler, N. (2015). Perspective: Concepts of printing technologies for oral film formulations. *International Journal of Pharmaceutics*, 494 (2), 578–584.

Preis, M., Eckert, C., Häusler, O., Breitkreutz, J. (2014). A comparative study on solubilizing and taste-masking capacities of hydroxypropyl-β-cyclodextrin and maltodextrins with high amylose content. *Sensors and Actuators B: Chemical*, 193, 442–450.

Raghavachari, R. (2001). Near-infrared applications in biotechnology. *Marcel Dekker Inc.*, New York, USA.

Raijada, D., Genina, N., Fors, D., Wisaeus, E., Peltonen, J., Rantanen, J., Sandler, N. (2013). A step toward development of printable dosage forms for poorly soluble drugs. *Journal of Pharmaceutical Sciences*, 102 (10), 3694–3704.

Reich, G. (2005). Near-infrared spectroscopy and imaging: basic principles and pharmaceutical applications. *Advanced Drug Delivery Reviews*, 57 (8), 1109–1143.

Rinnan, A., van den Berg, F., Engelsen, S.B. (2009). Review of the most common pre-processing techniques for near-infrared spectra. *TrAC Trends in Analytical Chemistry*, 28 (10), 1201–1222.

Rius-Ruiz, F.X., Crespo, G.A., Bejarano-Nosas, D., Blondeau, P., Riu, J., Rius, F.X. (2011). Potentiometric strip cell ased on carbon nanotubes as transducer layer: toward low-cost decentralized measurements. *Analytical Chemistry*, 83 (22), 8810–8815.

Rosenberg, J.M., Nathan, J.P., Plakogiannis, F. (2002). Weight Variability of Pharmacist-Dispensed Split Tablets. *Journal of the American Pharmaceutical Association*, 42 (2), 200–205.

Ross, S., Scoutaris, N., Lamprou, D., Mallinson, D., Douroumis, D. (2015). Inkjet printing of insulin microneedles for transdermal delivery. *Drug Delivery and Translational Research*, 5 (4), 451–461.

Sadeghi-Bazargani, H., Bangdiwala, S.I., Mohmmadi, R. (2011). Applicability of new supervised statistical models to assess burn injury patterns, outcomes, and their interrelationship. *Annals of Burns and Fire Disasters*, 24 (4), 191–198.

Salem, A.A., Barsoum, B.N., Izake, E.L. (2003). Potentiometric determination of diazepam, bromazepam and clonazepam using solid contact ion-selective electrodes. *Analytica Chimica Acta*, 498 (1-2), 79–91.

Sandler, N., Maattanen, A., Ihalainen, P., Kronberg, L., Meierjohann, A., Viitala, T., Peltonen, J. (2011). Inkjet printing of drug substances and use of porous substrates-towards individualized dosing. *Journal of Pharmaceutical Sciences*, 100 (8), 3386–3395.

Savitzky, A., Golay, M.J.E. (1964). Smoothing and Differentiation of Data by Simplified Least Squares Procedures. *Analytical Chemistry*, 36 (8), 1627–1639.

Scarpa, M., Stegemann, S., Hsiao, W.-K., Pichler, H., Gaisford, S., Bresciani, M., Paudel, A., Orlu, M. (2017). Orodispersible films: Towards drug delivery in special populations. *International Journal of Pharmaceutics*, 523 (1), 327–335.

Schiele, J.T., Quinzler, R., Klimm, H.-D., Pruszydlo, M.G., Haefeli, W.E. (2013). Difficulties swallowing solid oral dosage forms in a general practice population: prevalence, causes, and relationship to dosage forms. *European Journal of Clinical Pharmacology*, 69 (4), 937–948.

Scoutaris, N., Alexander, M.R., Gellert, P.R., Roberts, C.J. (2011). Inkjet printing as a novel medicine formulation technique. *Journal of Controlled Release*, 156 (2), 179–185.

Scoutaris, N., Ross, S., Douroumis, D. (2016). Current Trends on Medical and Pharmaceutical Applications of Inkjet Printing Technology. *Pharmaceutical Research*, 33 (8), 1799–1816.

Shah, R.B., Collier, J.S., Sayeed, V.A., Bryant, A., Habib, M.J., Khan, M.A. (2010). Tablet splitting of a narrow therapeutic index drug: a case with levothyroxine sodium. *AAPS PharmSciTech*, 11 (3), 1359–1367.

Shamsipur, M., Jalali, F., Haghgoo, S. (2002). Preparation of a cimetidine ion-selective electrode and its application to pharmaceutical analysis. *Journal of Pharmaceutical and Biomedical Analysis*, 27 (6), 867–872.

Solomon, L., Kaplan, A.S. (2007). Method of administering a partial dose using segmented pharmaceutical tablet. US0031494. (24.05.2017).

Stenlund, H., Johansson, E., Gottfries, J., Trygg, J. (2009). Unlocking interpretation in near infrared multivariate calibrations by orthogonal partial least squares. *Analytical Chemistry*, 81 (1), 203–209.

Sundfors, F., 2010. Solid-contact ion sensors: Materials and properties. Åbo Akademi University, Turku, xv, 85.

Tanner, S., Wells, M., Scarbecz, M., McCann, B.W., S.R. (2014). Parents' understanding of and accuracy in using measuring devices to administer liquid oral pain medication. *Journal of the American Dental Association*, (1939) 145 (2), 141–149.

Teng, J., Song, C.K., Williams, R.L., Polli, J.E. (2002). Lack of Medication Dose Uniformity in Commonly Split Tablets. *Journal of the American Pharmaceutical Association*, (1996) 42 (2), 195–199.

The White House, Office of the Press Secretary. (2015). FACT SHEET: President Obama's Precision Medicine Initiative. Available from: https://www.whitehouse.gov/the-press-office/2015/01/30/fact-sheet-president-obama-s-precision-medicine-initiative (31.10.16).

Trussell, H., Saber, E., Vrhel, M. (2005). Color image processing: Basics and special issue overview. *IEEE Signal processing magazine*.

Trygg, J., Wold, S. (2002). Orthogonal projections to latent structures (O-PLS). J. *Chemometrics*, 16 (3), 119–128.

Wickstrom, H., Nyman, J.O., Indola, M., Sundelin, H., Kronberg, L., Preis, M., Rantanen, J., Sandler, N., 2017. Colorimetry as Quality Control Tool for Individual Inkjet-Printed Pediatric Formulations. AAPS PharmSciTech 18 (2), 293–302.

Tufts Center for the Study of Drug Development. (2015). Personalized medicine gains traction but still faces multiple challenges, *Impact Reports*, Vol. 17 No. 3.

Uddin, M.J., Scoutaris, N., Klepetsanis, P., Chowdhry, B., Prausnitz, M.R., Douroumis, D. (2015). Inkjet printing of transdermal microneedles for the delivery of anticancer agents. *International Journal of Pharmaceutics*, 494 (2), 593–602.

Visser, J.C., Woerdenbag, H.J., Hanff, L.M., Frijlink, H.W. (2017). Personalized Medicine in Pediatrics: The Clinical Potential of Orodispersible Films. *AAPS PharmSciTech*, 18 (2), 267–272.

Vivó-Truyols, G., Schoenmakers, P.J. (2006). Automatic selection of optimal Savitzky-Golay smoothing. *Analytical Chemistry*, 78 (13), 4598–4608.

Walsh, J., Cram, A., Woertz, K., Breitkreutz, J., Winzenburg, G., Turner, R., Tuleu, C. (2014). Playing hide and seek with poorly tasting paediatric medicines: do not forget the excipients. *Advanced Drug Delivery Reviews*, 73, 14–33.

Wesołowska-Andersen, A. (2012). From genomic variation to personalized medicine, *Doctoral thesis*, Lyngby, Denmark. 152 pp.

Wickstrom, H., Nyman, J.O., Indola, M., Sundelin, H., Kronberg, L., Preis, M., Rantanen, J., Sandler, N. (2017). Colorimetry as Quality Control Tool for Individual Inkjet-Printed Pediatric Formulations. *AAPS PharmSciTech*, 18 (2), 293–302.

Wickstrom, H., Palo, M., Rijckaert, K., Kolakovic, R., Nyman, J.O., Maattanen, A., Ihalainen, P., Peltonen, J., Genina, N., Beer, T. de, Lobmann, K., Rades, T., Sandler, N. (2015). Improvement of dissolution rate of indomethacin by inkjet printing. *European Journal of Pharmaceutical Sciences*, 75, 91–100.

Woertz, K., Tissen, C., Kleinebudde, P., Breitkreutz, J., 2011. A comparative study on two electronic tongues for pharmaceutical formulation development. Journal of pharmaceutical and biomedical analysis 55 (2), 272–281.

Yu, L.X., Amidon, G., Khan, M.A., Hoag, S.W., Polli, J., Raju, G.K., Woodcock, J. (2014). Understanding pharmaceutical quality by design. *The AAPS Journal*, 16 (4), 771–783.

Zhang, H., Zhang, J., Streisand, J.B. (2002). Oral mucosal drug delivery: clinical pharmacokinetics and therapeutic applications. *Clinical Pharmacokinetics*, 41 (9), 661–680.

Zhou, L., Vogt, F.G., Overstreet, P.-A., Dougherty, J.T., Clawson, J.S., Kord, A.S. (2011). A Systematic Method Development Strategy for Quantitative Color Measurement in Drug Substances, Starting Materials, and Synthetic Intermediates. *The Journal of Pharmaceutical Innovation*, 6 (4), 217–231.

Zidan, A.S., Rahman, Z., Habib, M.J., Khan, M.A. (2010). Spectral and spatial characterization of protein loaded PLGA nanoparticles. *Journal of Pharmaceutical Sciences*, 99 (3), 1180–1192.

Publication bibliography

Hossein Vakili

Application of Analytical Techniques in Quality Control of Printed Pharmaceutical Dosage Forms

A Summary in Swedish

Vissa patientgrupper, t.ex. barn, behöver en mycket specifik dos av ett läkemedel för att nå en optimal terapeutiskt effekt. Därför behöver läkemedelsdosen i läkemedlet justeras specifikt för patienten. I den här avhandlingen undersöktes hur utskriftsteknologier kan användas i dosering av läkemedel och kombineras med lämpliga kvalitetskontrollsmetoder. Bläckstråleskrivarteknik erbjuder en lösning för att producera sådana precisionsmediciner. Läkemedlet löses i ett lämpligt lösningsmedel och hälls i bläckpatronen i en skrivare. Därefter produceras läkemedlet genom tryckning på ätbara substrat eller filmer. Läkemedelsdosen kan justeras med hög noggrannhet och reproducerbarhet på dessa tunna, stämpellika läkemedel som placeras i munnen och löses upp snabbt. Produktionshastigheten för dessa läkemedel är högt och tillverkningen behöver därför kombineras med snabba men pålitliga analysmetoder för kvalitetskontroll.

I optimala fall kunde denna småskaliga teknologi användas som en produktionslinje inom läkemdelsindustrin eller på apoteket där läkemedlet kunde tryckas direkt för patienten. Kvalitetskontrollmetoderna som undersöktes baserar sig bl.a. på spektroskopi och kolorimetri med vilka man mäter intensiteten av det reflekterade ljuset eller färgen från ytan av de utskrivna läkemedlen utan att röra provet. På så sätt förstör inte den använda metoden läkemedlet när den analyseras. Förändringarna i ljus- och färgintensiteten kan relateras till läkemedelsmängden och dess fysikaliska egenskaper. I avhandlingen undersöktes fördelarna och nackdelarna av de olika analytiska metoderna. Arbete visar tydligt att utskrifteknologier som används i kombination med lämpliga kvalitetskontrollsmetoder har stor potential att möjliggöra personaliserad dosering av läkemedel i framtiden.

ISBN 978-952-12-3659-4